THESIS

CHANGING DOGMA REGARDING THE CONFORMATION OF ELECTRON TRANSFERRING MENAQUINONE (MK)

Submitted by

Estela Serrano Magallanes

Department of Chemistry

In partial fulfillment of the requirements

For the Degree of Master of Science

Colorado State University

Fort Collins, Colorado

Spring 2017

Master's Committee:

Advisor: Debbie C. Crans

Carmen S. Menoni
Susan Tsunonda

ABSTRACT

CHANGING DOGMA REGARDING THE CONFORMATION OF ELECTRON TRANSFERRING MENAQUINONE (MK)

Menaquinone-9 (MK-9) is the natural substrate containing a naphthoquinone and an isoprenyl side-chain with nine isoprene units that carry out the electron transfer for the *Mycobacterium tuberculosis.* We present studies aiming to understand the chemical and biochemical properties of hydrophobic MK molecules. Specifically, we are investigating the MK derivative with two isoprene units, MK-2, because it provides us with the base structure containing the naphthoquinone unit and the isoprene side-chain. Its synthesis is relatively simple because the precursors are commercially available, which allows for large scale preparation and detailed characterization of the molecular structure under different conditions. Using 1D and 2D ^{1}H NMR studies we are establishing that *MKs have different conformations depending on the specific environmental conditions.* Similarly, we show using ^{1}H-^{1}H 2D NOESY NMR studies that *the association of MK with the surfactant- water interface of reverse micelles, which is a model membrane system, modify the conformation of the menaquinone derivative.* Finally, the redox potentials of MK-2 was measured in the three different solvents (DMSO, CH_3CN and pyridine). *We hypothesize that the redox potential is correlated to the conformational of the MK.* We observed that the redox potentials varied with solvent. The observed folded structures of MK derivatives stand in contrast to the linear conformation shown in life science text books.

ACKNOWLEDGEMENTS

I would like to thank Dr. Crans who provided invaluable support and guidance in this crazy world we call Graduate School. I also would like to thank all the members of the Crans group for their efforts in making all my presentations the best that they could be. I would also like to specifically acknowledge: Jordan T. Koehn for his work on the synthesis of MK-2 and for his work on the ^{1}H-^{1}H 2D NOESY NMR of MK-2; Benjamin J. Peters for his work on the ^{1}H-^{1}H 2D NOESY NMR of the reverse micelles, the Molecular Mechanics and the Langmuir Though experiments; and Cheryle N. Beuning for her work on the Electrochemistry of MK-2.

DEDICATION

To: Dr. Adela Magallanes, Cecilia Magallanes, Hector Magallanes, and Mary J. Fisher. Without your continued support whether it be emotional, educational, vocational, etc. I would not be getting this degree.

TABLE OF CONTENTS

LIST OF FIGURES

LIST OF ABBREVIATIONS

ACETONITRILE ..... CH_3CN

BENZENE-d_6 ..... C_6D_6

BORON TRIFLUORIDE ..... BF_3

CHLOROFORM-d ..... $CDCl_3$

COMPRESSION MODULUS ..... C_S^{-1}

CONFIDENCE INTERVAL CI

CYCLIC VOLTAMMETRY CV

DEUTERIUM OXIDE ..... D_2O

DIMETHYLFORMAMIDE ..... DMF

DIMETHYLSULFOXIDE ..... DMSO

DIMETHYLSULFOXIDE-d_6 ..... d_6-DMSO

1,2-DIPALMITOYL-SN-GLUCERO-3-PHOSPHOCHOLINE ..... DPPC

1,2-DIPALMITOYL-SN-GLYCERO-3-PHOSPHOETHANOLAMINE ..... DPPE

DIRECT ANALYSIS IN REAL TIME ..... DART

DOUBLE DEIONIZED WATER ..... DDI H_2O

DYNAMIC LIGHT SCATTERING ..... DLS

ELECTRON SPRAY IONIZATION MASS SPECTROMETRY ..... ESI MS

ELECTRON TRANSPORT SYSTEM ..... ETS

ETHYL ACETATE ..... EtoAc

FERROCENE ..... Fc

HALF-WAVE POTENTIAL ..... $E_{1/2}$

HIGH RESOLUTION MASS SPECTROMETRY.....HRMS

LIQUID CHROMATOGRAPHY/MASS SPECTROMETRY..... LCMS

LOWEST UNOCCUPIED MOLECULAR ORBITAL..... LUMO

LOW RESOLUTION MASS SPECTROMETRY ..... LRMS

MENAQINONE..... MK

MENAQINONES..... MKs

MENAQUINONE-2.....MK-2

MENAQUINONE-4.....MK-4

MENAQUINONE-9.....MK-9

MERCK MOLECULAR FORCE FIELD 94.....MMFF94

NUCLEAR OVERHAUSER EFFECT SPECTROSCOPY.....H^1-H^1 NOESY

POLYDISPERSITY INDEX..... PDI

PROTON NUCLEAR MAGNETIC RESONANCE .....H^1 NMR

REVERSE MICELLE .....RM

SILVER NITRATE.....$AgNO_3$

SODIUM BICARONATE ..... $NaHCO_3$

SODIUM SULFATE..... $NaSO_4$

SULFOSUCCINATE SODIUM SALT.....AOT

SURFACE AREA ..... A

SURFACE PRESSURE .....π

TETRABUTYLAMMONIUM .....TBAP

TETRAMETHYLSILANE ..... TMS

CHAPTER ONE: CHARATERIZATION ON MENAQUINONE-2 (MK-2)

INTRODUCTION

Small hydrophobic molecules called lipoquinones play key roles in the respiratory electronic transport systems (ETS) of prokaryotes and eukaryotes.[1-4] Part of the electron transfer complex, a membrane associated protein called MenJ uses MK-9 as a part of respiration and oxidative phosphorylation which happens in the membrane.[5] These roles contribute to the separation of charge across the membrane by shuttling electrons between protein complexes and act as electron donors and acceptors.[1-3] MKs have a structure that contains a naphthoquinone and an isoprenyl side-chain of varying length and degree of regiospecific saturation as seen is Fig. 1, pg. 26.[3, 6-7] Although much is known about the function of MK-9 and analogs, limited information is available on the chemical and physical properties of MK molecules. It is generally accepted that MKs are located in the membrane, but their structural and conformational detail has not been characterized. As a consequence, menaquinone derivatives are depicted as "Q" in textbooks and in the general literature overall.[4, 8-9]

Although conformational analysis of alkanes and alkenes are fundamental and basic for understanding simple organic molecules, little information is available on the actual conformation of compounds such as MKs. This lack of information is in part because they are not soluble in aqueous solution and because their hydrophobic environment in biological systems is not well defined. Dogma suggest that the all-trans geometries are most stable,[10] however, considering the entropic contributions to the energy, gauche arrangements are often

energetically equality favorable because of entropic contributions. This is in part due to the spatial requirements that all molecules exert and can be justified using limited sphere-considerations. [11] The shapes and conformational properties of other groups of linear hydrophobic aliphatic compounds, like fatty acids, have been reported. Fatty acids, are found to exist as either straight chains or folded conformations depending on structural details and environmental conditions. Based on this precedent *we hypothesize that MKs will have different conformations depending on the specific environmental conditions.* We investigated this hypothesis using 1D and 2D NMR spectroscopy.

However, detailed analysis by Law and coworkers of long chain allylic polyunsaturated fatty acid chains using Hartree-Fock calculations showed that differences between the all-trans and helical folded structures are only a few kcal/mol.[12] These studies are consistent with previous work carried out with fatty acids where the experimental studies showed that the conformations of fatty acids can and do change with changes in the external conditions such as pressure.[13] *We hypothesize that the association of MKs with the membrane will influence the conformation of the MK derivative.* We investigated this question using spectroscopic methods in two simple model membrane systems, the reverse micelle and the Langmuir monolayers.

Several model membranes exist, ranging from the more complex cell like models to less complex where many of the proteins have been removed such as liposomes, micelles and reverse micelles. We are interested in characterizing the molecular details of the location and association with the interface; therefore, we selected the reverse micellar model in association with a Langmuir monolayer system.[14-18] The former is a ternary microemulsion system in which a surfactant is dissolved in an organic solvent, and the addition of water creates nanosized

water droplets encased in surfactant like the one see in Fig. 2, pg. 27.[16, 18-21] The interface of the RM provide a simple model that mimics the interface in biological membranes.[22] NMR spectroscopy of the RM can provide molecular detail of location of the MK.[23-25] This approach is desirable particularly when these studies are accompanied by a more common membrane model system such as the Langmuir monolayers.[14, 26]

The role of MK derivatives in the membrane as an electron carrier, requires that it associates with proteins involved in the electron transfer process.[27] However the details of the association of MK, electron transfer proteins and the membrane are not well understood.[28] Therefore, information on how the electron donor properties of MK changes with environment is very valuable. MKs undergo two one electron reduction processes forming first the radical anion (semiquinone) and then a dianion.[29-31] These processes are described extensively in the literature and redox potential of a range of MK derivatives have been reported under a range of conditions.[29-31] Therefore, linking the conformational properties with the reactivity, *we hypothesize that the redox potential can be associated with the conformation of MK*. We have investigated the redox properties of a simple MK, MK-2, under conditions where we have characterized both its structure and its redox properties.

In the following manuscript, we have synthesized and characterized a small MK derivative, with two isoprene units, MK-2. We investigated the structure and electrochemistry of this compound beginning in different organic solvents and extending the studies to a simple membrane model system.

EXPERIMENTAL SECTION

General Materials

Menadione (crystalline), sodium hydrosulfite (85.0%), 1,4 dioxane (99.9%), BF_3 etherate (≥46.5%), dioctyl sulfosuccinate sodium salt (AOT, 97.0%), isooctane (2,2,4-trimethylpentane, ≥99.0%), chloroform (99.8%), methanol (99.9%), disodium phosphate (anhydrous), trisodium phosphate (96.0%), tetrabutylammonium perchlorate (TBAP, ≥ 99.0%), ferrocene (Fc, anhydrous), silver nitrate ($AgNO_3$, ≥ 99.0%), and activated charcoal were purchased from Sigma Aldrich. Absolute ethanol and ultra-high purity argon gas (99.9%) were acquired from Pharmco-Aaper and Airgas, respectively. Deuterated solvents of acetonitrile (CH_3CN) (D 99.8%), dimethyl sulfoxide (DMSO) (D 99.9%, + 0.05% V/V tetramethylsilane), and deuterium oxide (D_2O, 99.9%) were acquired from Cambridge Isotope Laboratories, Inc. Deuterated pyridine (D 99.8%) was purchased from Arcos Organics. DPPC (1,2-dipalmitoyl-sn-glycero-3-phosphocholine, ≥ 99.0%) and DPPE (1,2-dipalmitoyl-sn-glycero-3-phosphoethanolamine, ≥ 99.0%) were purchased from Avanti Polar Lipids Inc. MK-2 was prepared as stated in the synthesis section and treated as a lipid within these experiments. Double Deionized Water (DDI H_2O) was purified with a Barnstead E-pure system (18.2 MΩ-cm). All chemicals were used without purification except AOT, and the organic solvents. AOT was purified by using previously reported methods.[32]

General Methods

MK-2 is synthesized using the approach shown in Scheme 1 adapted from a published procedure by Payne et al. and Suhara et al.[33-34] All non-aqueous reactions were carried out under an atmosphere of argon and flame-dried glassware and were stirred using a magnetic stir

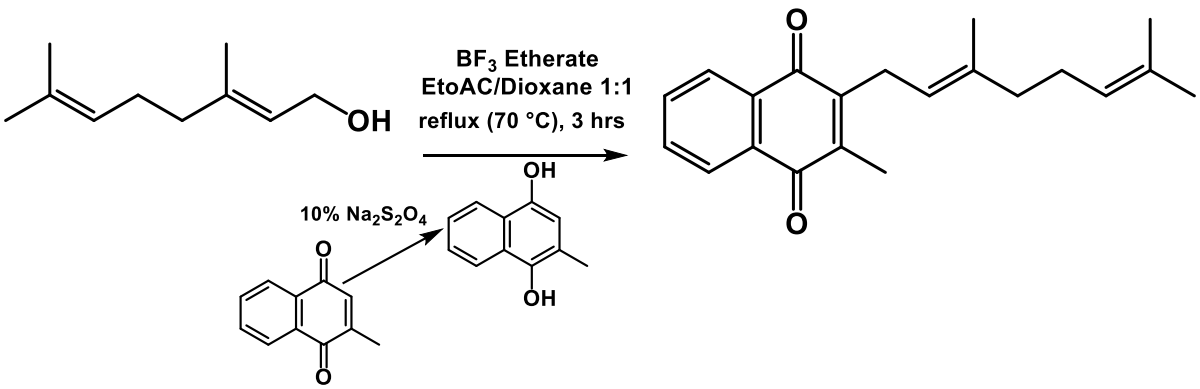

Scheme 1. Synthetic scheme for MK-2 reported first by Payne, Suhara and coworkers.

plate using anhydrous solvent unless otherwise noted. All reactions were monitored by thin layer chromatography (TLC) on Whatman Partisil® K6F TLC plates (silica gel 60 Å, 0.250 mm thickness) and visualized using a UV lamp (366 or 254 nm). Products were purified by flash chromatography (SiliCycle®SiliaFlash® F60, 43-60 μm 60 Å). Yields refer to chromatographically and spectroscopically (^{1}H NMR) homogenous materials unless otherwise noted.[34] Organic solvents acetonitrile (CH_3CN), dimethyl sulfoxide (DMSO), and pyridine were purified by distillation then dried over activated 3 Å molecular sieves (40 g / 200 mL solvent) for at least 3 days before use.

MK-2 Synthesis

To a 500 mL Schlenk flask was added a stir bar, 100 mL diethyl ether, and 5 g menadione (29 mmol). Then, 100 mL of 10% aq. of $Na_2S_2O_4$ (57.4 mmol) was added and the solution immediately turned dark red. After 30 mins of stirring at ambient temperature the solution was a clear yellow. The aqueous layer was separated and extracted with diethyl ether (3X 100 mL). The aqueous layer was washed with 100 mL sat. $NaHCO_3$, followed by DDI H_2O (2X 100 mL), and lastly by 100 mL brine. After washing with brine, the aqueous layer was dried with $Na_2S_2O_4$ and concentrated under reduced pressure. The crude powder was titrated with 50

mL of pentane, vacuum filtered and washed with 100 mL of pentane to yield 4.25 g pale purple solid. Menadiol formation is indicative by ^{1}H NMR ($CDCl_3$) by presence of a peak at 6.65 ppm and absence of a peak at 6.83 ppm consistent with literature.[35]

To a 100 mL Schlenk flask was added 16 mL of ethyl acetate and 16 mL of dry 1,4-dioxane which was purged/evacuated with argon repeatedly. Then 2.5 g crude menadiol (4:1 menadiol:menadione by NMR integration, 11.5 mmol) was added and then to this 60 °C stirring solution was added 1.92 g (12.5 mmol) geraniol followed by the drop wise addition of 0.8 mL fresh BF_3 etherate. The solution was allowed to reflux at 70-72 °C for 3 hrs. under argon. The dark orange colored reaction was quenched with 100 mL of ice H_2O and then extracted with diethyl ether (3X, 100 mL). The yellow organic extracts were washed with 100 mL of sat. $NaHCO_3$, 100 mL DDI H_2O followed by washing with 100 mL brine, then dried with Na_2SO_4, and concentrated to yield 3.71 g of crude red oil. The crude oil was purified by flash column chromatography (1000 mL 230-400 mesh SiO_2, 70 mm column, 20:1 pentane/ethyl acetate). The yellow oil obtained was dried under reduced pressure overnight to yield 0.71 g (2.31 mmol, 19.2% yield) as yellow solid. The scale of this reaction was 14 times larger than the reported synthesis. ^{1}H NMR (400 MHz, DMSO) δ: 7.97-8.00 (m, 2H), 7.80-7.85 (m, 2H), 5.01 (t, J=8 Hz, ^{1}H), 3.30 (d, 2H, J=4 Hz), 2.11 (s, 3H), 1.75 (s, 3H), 1.65 (s, 3H). ^{13}H NMR (400 MHz, DMSO) δ: 184.65, 183.86, 145.13, 142.91, 133.83, 131.55, 131.51, 125.87, 125.80, 119.44, 25.60, 25.45, 17.87, 12.40. LRMS (ESI 70 eV, EtoAC) calcd for $C_{16}H_{16}O_2$ [M^+] 240.12, found 240.10. HRMS (DART) calcd for $C_{16}H_{16}O_2$ [$(M+H)^+$] 241.1223, found 241.1175.

NMR studies

1D and 2D ^{1}H studies were carried out both in organic solvents and more complex media (see below for RM studies). ^{1}H and ^{13}C spectra were recorded using a Varian Model MR400 operating at 400 or Model Inova operating at 400 MHz and 100 MHz. Chemical shift values (δ) are reported in ppm and referenced against the solvent peaks in ^{1}H NMR (d_6-DMSO, δ at 2.51 ppm; $CDCl_3$, δ at 7.26 ppm; C_6D_6 at 7.16 ppm) and in ^{13}C NMR (d_6-DMSO, δ at 39.52 ppm). All NMR spectra were recorded at 22 °C.

Sample preparation for NMR Studies Reverse micelles (RMs)

A 0.5 M AOT stock solution was made by dissolving AOT (5.56 g, 12.5 mmol) in isooctane (25 mL). RMs were prepared by mixing the 0.5 M AOT stock solution with a D_2O (pH 7), and then vortexed until clear. MK-2 RMs were made in a similar manner except an 11.2 mM MK-2 stock solution was prepared by directly dissolving MK-2 in the 0.5 M AOT/isooctane solution. Then the MK-2-AOT-isooctane stock solution along with D_2O (pH 7) were used to make RMs.

1D ^{1}H NMR of AOT/isooctane RMs that Contain MK-2

1D ^{1}H NMR experiments were run using a Varian Inova 400 MHz instrument using routine parameters (pulse angle: 45°, RD: 1 s). The RM spectra were referenced using the isooctane methyl peak set to at 0.904 ppm.[36] Data analysis and spectrum workup was done using the NMR software, MestReNova version 10.0.1.

Sample Preparation for ^{1}H-^{1}H 2D NOESY NMR Solution Studies in benzene and DMSO

A 100 mM MK-2 solution, was prepared by dissolving MK-2 (0.0154 g) in deuterated benzene (0.5 mL). A 67 mM MK-2 solution was prepared by dissolving MK-2 (0.0154 g) in deuterated DMSO (0.75 mL).

^{1}H-^{1}H 2D NOESY NMR studies in benzene and DMSO

A NOESY sequence of 200 transients in the f1 dimension with 32 scans pre transient and a 500 ms mixing time was used. The NMR was locked on the deuterium signal from benzene or DMSO and the spectrum was reference to the solvent peak. The spectrum was analyzed with MestReNova version 10.0.1 NMR processing software.

Sample preparation for 2D NMR (^{1}H-^{1}H NOESY) Studies (RMs)

To prepare the AOT/isooctane stock solution, 0.22 g AOT (0.5 mmol) was dissolved into isooctane (1 mL) for a final 0.5 M AOT stock solution. Then 0.035 g (1.1 mmol) of MK-2 was dissolved into the 0.5 M AOT stock solution for a final concentration of 110 mM MK-2. This final mixture results in a w_0 12 RM microemulsion with an overall concentration of MK-2 being 100 mM (29 molecules per RM).

^{1}H-^{1}H 2D NOESY NMR in AOT/isooctane RM

As previously mentioned, MK-2 containing RMs were prepared by directly dissolving MK-2 in the AOT stock solution. A standard NOESY pulse sequence of was used (See ^{1}H-^{1}H 2D NOESY studies in Benzene and DMSO). The NMR was locked onto the D_2O peak and the spectrum was referenced to the isooctane methyl peak at 0.904 ppm as previously reported.[36] The resulting spectrum was processed using MestreNova NMR processing software version 10.0.1. The 3D structure illustration within a RM was drawn using ChemBioD Ultra 12.0 and ChemBio3D Ultra 12.0 based on spectral parameters described under results.

Sample preparation for electrochemical studies 1D ^{1}H NMR of MK-2

Samples prepared with and without TBAP in either DMSO, C_6D_6, or d_5-pryidine with 15-20 mg of MK-2. This was done to determine if the presence of 0.1 M TBAP affected the

observed chemical shifts of MK-2's protons. The spectra were referenced by internal TMS at 0.00 ppm. The presence of electrolyte had no measureable effect on the chemical shifts of MK-2.

Mass Spectrometry

Low resolution mass spectrometry (LRMS) experiments were conducted by Electron Spray Ionization Mass Spectrometry (ESI MS) on an Agilent technologies 6130 Quadrupole LCMS. High resolution mass spectrometry (HRMS) experiments were conducted by Direct Analysis in Real Time (DART) on an Agilent 6220 TOF LCMS interfaced to an Agilent 1200 with a DART source.

Molecular Dynamics and Structure Comparison

Merck Molecular Force Field 94 (MMFF94) molecular dynamics gas phase simulations were conducted using ChemBio3D Ultra 12.0 at 25°C. The simulations were run for up to 10,000 iterations. A distinct conformation was minimized and a MMFF994 energy calculation was run using up to 500 iterations with a root mean square gradient of 0.001. For a full table of structural parameters such as the distances between hydrogen atoms within the structures and energies calculated for each of the 3D conformation can be found in the appendix.

RM Sample Preparation for Dynamic Light Scattering (DLS) Studies

RMs were prepared as above except that DDI H_2O was used as the water pool instead of D_2O and the 0.5 M AOT/RM was diluted to a 0.1 M AOT/RM solution with isooctane after the RMs were formed.

DLS Measurements

The hydrodynamic radius of the RMs was determined by DLS measurements performed on a Malvern Zetasizer Nano ZS instrument (Malvern Instruments, Malvern, UK). The DLS cuvette (1 cm X 1 cm, glass) was washed out 3 times with isooctane followed by 3 washes with the RM sample. Then, the cuvette was filled with 1 mL of the RM sample and closed with a Teflon cap. Each experiment was done at 22 °C and consisted of a 700 sec sample equilibration period followed by 10 measurements made each of 15 scans.[26] Each sample was done in triplicate. The diameter, polydispersity index (PDI) were recorded (see appendix) and compared to literature. The data was analyzed using Malvern DLS Software.

Langmuir Monolayer Formation

The sub-phase for each experiment consisted of approximate 50 mL a 20 mM sodium phosphate buffer (pH 7.4). The lipid solution was prepared by dissolving powdered lipid into a chloroform:methanol (9:1, v:v) solution to produce 1 mM lipid. The film applied to the subphase consisted of 20 µL of lipid or a 50:50 mol fraction mixture of MK-2 with DPPC (or DPPE). The resulting film was equilibrated for 15 minutes and then compressed using a Teflon ribbon at a rate of 10 mm/min (2.4 $Å^2$/chain). The surface pressure was measured using the Wilhemy plate method where a wire probe was used as the plate on a Kibron µTrough XS.[37] The compression modulus was calculated using Eq. 1 from the average compression isotherm results using Origin Pro Version 9.1 where C_s^{-1} is the compression modulus, A is the trough surface area, and π is the surface pressure.[14]

(1). $$C_s^{-1} = -A\left(\frac{d\pi}{dA}\right)$$

Electrochemistry

All electrochemistry was performed on a CHI 750D potentiostat. For the cyclic voltammetry (CV) a classical three electrode system was used with scan rate of 100 mV/s at ambient room temperature. The glassy carbon working electrode (BASi MF2012, 3 mm) was lightly polished between runs with alumina powder then rinsed with water and ethanol. The platinum wire counter electrode (BASi MW1032) was gently polished between runs with 600 grit sandpaper. The Ag^+/Ag reference electrode (BASi MW1085) was constructed by using the Ag wire gently polished with 600 grit sandpaper inserted into a freshly prepared solution of organic solvent (CH_3CN, DMSO, or pyridine) with 0.1 M TBAP and 0.01 M $AgNO_3$. Before the CV was recorded the reference electrode equilibrated in the 2 mM MK-2 with 2 mM Fc in the same organic solvent for 10 minutes with bubbling argon gas to degas any O_2. All half-wave potentials recorded were referenced to the Fc^+/Fc couple in the respective solvent, this was achieved by subtracting the Fc^+/Fc couple from calculated half wave potentials. After drying the solvent, the Fc^+/Fc couple against the Ag^+/Ag couple in CH_3CN, DMSO and pyridine was measured in quadruplicate and the Fc^+/Fc couple against the Ag^+/Ag couple in CH_3CN was 0.080 V ± 0.006 V in DMSO 0.171 V ± 0.002 V and in pyridine 0.563 V ± 0.003 V.

(2). $E_{1/2} = \frac{E_{pc}+E_{pa}}{2}$

(3). $\Delta E_p = E_{pc} - E_{pa},\ n = x * \frac{0.059\ V}{\Delta E_p}$

The half wave potentials were calculated using equation 2 where E_{pc} and E_{pa} are the cathodic and anodic peak potentials, respectively. The i_{pc} and i_{pa} were measured manually with a ruler on the CV's in cm. The number of electrons, n, in each process were determined using equation 3,

where x is the adjustment factor in each solvent determined by setting the standard ferrocene *n*=1 as the ΔE_p(difference between cathodic and anodic peaks) in non-aqueous solutions.

RESULTS AND DISCUSSION

MK-2 Synthesis

MK-2 was synthesized using an adapted procedure from Suhara et al. and Payne et al. shown in Scheme 1.[32-34] This preparation led to a yield of 19.2%, which is lower than the reported deuterated MK-2 preparation.[34] The lower obtained yield could be possible due to the inherent difficulties in scaling up reactions.[38]

1D ^{1}H NMR of MK-2 in Different Solvents

MK-2 was first characterized using 1D ^{1}H NMR spectroscopy. Fig. 3, pg. 28 shows 1D ^{1}H NMR spectra of MK-2 from the bottom in D_2O, d_6-DMSO, d_6-benzene and isooctane. The observed chemical shifts of MK-2 varies dramatically in the different solvents shown. We examined hydrophobic (aliphatic (isooctane) and aromatic (d_6-benzene)) solvents as well as hydrophilic (d_6-DMSO and H_2O / D_2O) solvents. The spectra are all showing very different spectroscopic signatures. For example, the pairs of aromatic protons H_a/H_b and H_c/H_d are significantly different in the two different classes of solvents. This variation suggests that the conformation MK-2 in different solvent environments is changing.

Focusing on the 1D ^{1}H NMR spectra of MK-2 in two hydrophilic solvents, d_6-DMSO and D_2O, some differences and similarities are observed (Fig.3, pg. 28). The MK-2 spectrum in D_2O required significantly more scans because of the poor solubility in D_2O compared to d_6-DMSO. The protons are generally at further upfield shifts in D_2O presumably indicative of more

aggregation in this solvent. There are no H_h and H_i signals observed in the D_2O spectrum because of overlap with the HOD peak. Importantly, the HOD signal in the d_6-DMSO spectrum is observed at 3.3 ppm which allows for observation of the H_h and H_i signals at 4.9 ppm. The spectrum of MK-2 in d_6-DMSO also has some similarities to the MK-2 spectrum in D_2O. The aromatic protons on the menaquinone H_a/H_b are shifted about 0.2 ppm from the H_c/H_d signals in both solvents. This suggests a similar environment for these protons in these two solvents. Therefore, these two spectra combined provides a representation of the properties of the MK-2 in a hydrophilic environment.

Next, the aromatic and olefinic protons were compared in the hydrophobic solvents isooctane and d_6-benzene. In the isooctane and d_6-benzene spectra, the MK-2 peaks H_a, H_b, H_c, H_d, H_h, and H_i can be seen and readily identified. The signals from H_h and H_i are all further downfield compared to the signals in hydrophilic solvents. This is in contrast to the aliphatic protons in the spectrum in d_6-benzene which are very similar to those in d_6-DMSO. The changes in the chemical shifts are most distinctive in the aromatic and olefinic protons suggesting that there are some major differences in their respective environments. However, 2D NMR will be done to elucidate how much of this change in chemical shift is due to conformational changes and how much is due to the solvent affect. Combined these studies suggest that the conformation of MK-2 is very sensitive to its environment and more information on these conformations is sought using 2D NMR methods.

^{1}H-^{1}H 2D NOESY of MK-2 in d_6-benzene and d_6-DMSO

Fig. 4, pg. 29 shows the ^{1}H-^{1}H 2D NOSEY spectra in benzene and d_6-DMSO. The middle spectrum shows the full spectrum of MK-2 in benzene and the indicated sub-regions within this

spectrum are expanded as shown. The top left expanded spectra show that the H_h and H_i protons are in similar environments in benzene and d_6-DMSO. In both solvents, H_h and H_i interact with H_z, H_r, H_q and H_n/H_m. Furthermore, H_a and H_b interact with each other in both solvents. In addition, proton H_w interacts with protons H_h/H_i and H_m/H_n in benzene and d_6-DMSO both. In contrast, H_w does not interact with H_x, H_y and H_z in d_6-benzene, while in d_6-DMSO the H_w proton interacts with H_x, H_z, H_y, H_r and H_q. These results show that there are similar interactions between the aromatic and olefinic protons in the two solvents, however, there is a twist around the C-C bond leading to proximity of the H_w with the H_x, H_z, H_y, H_r and H_q protons. In place of simply drawing these structures per these descriptions, we used the Molecular Mechanics calculations to provide 3D images of the structures.

Molecular Mechanics of MK-2

Representation of the conformations of MK-2 is difficult because of MK-2's many degrees of freedom. Using Molecular Mechanics calculations, we explored the energy surface and some of the possible conformations that MK-2 can undertake as defined by the ^{1}H-^{1}H 2D NOESY experiments of MK-2 in d_6-DMSO and d_6-benzene. Possible structures and energies of MK-2 in the gas phase can be calculated with Molecular Mechanics. We did not attempt to describe this system (MK-2) completely using computations, we merely selected structures according to the ^{1}H-^{1}H 2D NOESY data in benzene and DMSO and structures with and without energy minimization commonly found in textbooks (Fig. 5, pg. 30). One of the low energy structures found for MK-2 (Fig. 5A, 60.5 kJ/mol, H_w-H_y: 2.60 Å), is consistent with the parameters observed for MK-2 in DMSO. Fig. 5B, pg. 30 shows a structure of MK-2 that is found in benzene (60.9 kJ/mol, H_w-H_y: 3.60 Å). Both these structures show folding of the isoprene unit

back over themselves. We compared these structures with another low energy structure that showed isoprene chain folding, however, this folding was away from the naphthoquinone unit (Fig. 5C, pg. 30).

We are interested in comparing the conformations of the MK-2 structure that is experimentally forming in benzene and DMSO with structures most commonly used when depicting MK in textbooks and the literature. The next set of structures, MK-2 (D-F) were therefore developed from the structures most often depicted by 2D drawings. The energies of these structures are between 3 and 62 kJ/mol higher than the energies of the MK-2 structures found in benzene and DMSO. A full table of conformational energies and proton distances of MK-2 can be found in the appendix. These studies demonstrate the need for further studies using more sophisticated computational methods.

As shown above, the MK-2 conformation is very sensitive to its environment. It was our intention to examine this smaller MK derivative first, because it provides the inherent properties of a molecule with the naphthoquinone and a small isoprene chain. As the length of the isoprene chain increases, its effects on the properties of the natural electron transfer agent, MK-9, are likely to increase. However, our studies so far demonstrate that MK-2 folds in a manner not previously recognized in the life sciences. Details regarding MK-9's electrochemistry and interactions with bacterial membranes is likely to be very important for facilitation of electron transfer. As a result, we investigated 1) how MK-2 interacted with simple model membrane systems and 2) the electrochemistry in organic solvents of the simple MK analog.

1D ^{1}H NMR of MK-2 in RM

MK is very sensitive to its environment, information is crucial for the understanding of the interactions of MK-2 in a model membrane system. Specifically, it will allow placement determination of MK-2 molecule in the inhomogeneous membrane-like environment. Fig. 6, pg. 31 shows a stack plot of the MK-2 aromatic protons (H_a/H_b and H_c/H_d) in D_2O or isooctane solutions of MK-2-RMs (AOT/isooctane microemulsions) of various sizes (w_0: 4, 8, 12, 16, and 20) for comparison with the empty AOT/isooctane RM. The aromatic MK-2 protons in the AOT/isooctane RMs are similar to the signals observed in isooctane and very different from the signals observed in D_2O. This similarity and difference can be seen in the distance between the aromatic protons (H_a/H_b and H_c/H_d) in isooctane, D_2O, and RM. The distance between H_a/H_b and H_c/H_d is 0.52 ppm in isooctane, 0.47 ppm in the RM and 0.27 ppm in D_2O. This suggests that the environment of MK-2 protons in AOT/isooctane RMs is more similar in environment to isooctane than D_2O. This is consistent with MK-2 associating more the AOT molecules than with the isooctane. As seen from the reference lines in Fig. 6, pg. 31, the chemical shift from the aromatic protons shifts to a lower ppm as the RM size increases. However, the chemical shift change for H_a/H_b is smaller than H_c/H_d. Therefore, the environment for H_a/H_b is not changing as much as the environment for H_c/H_d protons. This is consistent with H_a/H_b being in a slightly different environment that H_c/H_d. This is consistent with the location of H_c/H_d in the interface changing more than the location of H_a/H_b. However, before any specifics about the location of MK-2 within the interface can be discussed ^{1}H-^{1}H 2D NOESY NMR must be done, which will be addressed in the next section.

^{1}H-^{1}H 2D NOESY NMR of MK-2 in RM

To obtain further information on the location and conformation of MK-2 in RMs, we obtained the 2D ^{1}H-^{1}H NMR spectrum of MK-2. In Fig. 7, pg. 32, the interactions between MK-2's H_w proton with H_m are consistent with them being in the same plane (and not as depicted in Fig. 5E). The planarity of these protons would suggest MK-2's isoprene tail has a 90° angle with the naphthoquinone (as in structures Fig. 5A-D, pg. 30). Illustration of the structure supporting the interaction between H_w and H_q protons is shown in Fig. 8, pg. 33. The ^{1}H-^{1}H 2D NOESY spectrum in Fig. 7, pg. 32 favor an MK-2 conformation with the isoprene tail folding over on to the naphthoquinone. This folded conformation of MK-2 in RMs is similar to the conformations observed in organic solvents, where the naphthoquinone is planar and the isoprene tail folds over the planar naphthoquinone (Fig. 8, pg. 33)

^{1}H-^{1}H 2D NOESY NMR also provides information on the location of MK-2 in RMs. Fig. 9, pg. 34 shows the ^{1}H-^{1}H 2D NOESY spectrum of MK-2's aromatic protons in RMs. In this spectrum, MK-2 aromatic protons interact with AOT's H6, H8 and H10 protons. However, these interactions happen at slightly different chemical shifts (8.0 ppm for H_a/H_b and 7.6 ppm for H_c/H_d) suggesting that the environment is not the same for all the aromatic protons. Moving down the MK-2 molecule, MK-2 protons H_i and H_h interact with AOT's H3 and H4 protons. MK-2's H_m, H_n protons also interact with AOT's H3 proton. These interactions are consistent with MK -2 sitting in between the AOT tails with the methyl on the quinone portion of the naphthoquinone of MK-2 facing the RM interface and the benzene portion of the naphthoquinone facing the isooctane solution, see Fig. 10, pg. 35 for a schematic drawing.

Model Membrane System: Langmuir Trough

Langmuir monolayers were used to investigate the interactions of MK-2 with the interface. Fig. 11, pg. 36 shows the change in pressure as a function of area (Fig. 11 a, c, pg. 36) and the resulting compression moduli as a function of pressure (Fig. 11 b, d, pg. 36).

The compression isotherms of DPPC and DPPE, are similar to literature findings where there is a characteristic transition of the DPPC film at about 8 mN/m and collapsing at about 55 mN/m for both films.[39] The MK-2 films had a maximum surface pressure of about 20 mN. This result suggests either an unstable film or a collapse at low pressure. The compression isotherm of the mixture of DPPC and MK-2 shows a disappearance of the gas to liquid phase transition at 8 mN suggesting there is an interaction between MK-2 and DPPC. MK-2 brings the DPPC molecules closer together at low pressures. The presence of MK-2 also causes the collapse of the DPPC film at 50 mN/m compared to 55 mN/m. This suggests that MK-2 has a destabilization effect on the film. To understand the interactions of MK-2 with DPPE and DPPC further the compression moduli were calculated using equation 1. When comparing the compression moduli of DPPC or DPPE and lipid:MK-2 compression moduli, there is a clear decrease in compression modulus. A decrease in compression modulus has been attributed to an increase in compressibility.[40] This suggests that MK-2 causes the lipid films to compress earlier than the pure lipid counterparts.

In summary, the interactions between MK-2 and a DPPC/DPPE interface agree with what has been shown for quinones in literature.[9] These results along with the literature support an MK-2's interaction with the interface shown with RMs.[9] Further studies will be conducted using longer MK homologs.

Reactivity of different conformations: Electrochemistry

The electrochemistry of MK-2 in three different organic solvents was examined to determine if the differing conformations in these solvents could be correlated with the observed electrochemical potential. We were unable to perform electrochemistry of MK-2 in pure benzene due to the electrolyte's low solubility and therefore low conductivity in this solvent.[41] We then used pyridine as a replacement due to similar solvent properties. 1D ^{1}H NMR studies of MK-2 were done in solvents with and without the electrolyte in order to define the best conditions to carry out the redox chemistry. TBAP was chosen as the electrolyte

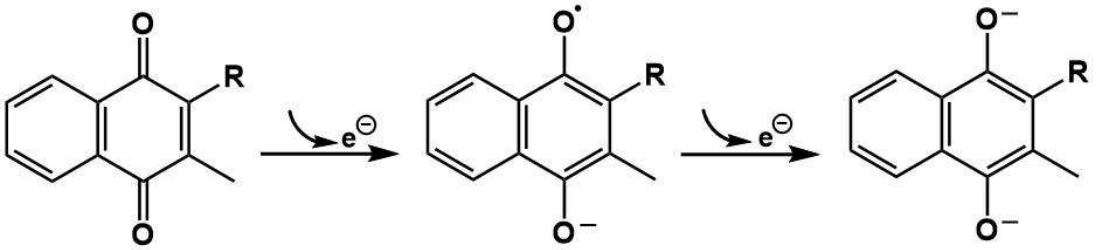

Scheme 2. The one electron reduction of the quinone (Q) to the semiquinone radical anion ($Q^{\bullet -}$) and the second one electron reduction to the dianion (Q^{2-}).

because the addition of TBAP to MK-2 solutions in each solvent did not affect the observed chemical shifts of the MK-2 protons and thus no evidence for ion pairing was found. Therefore, direct comparisons of 1D or 2D NMR data to that of the electrochemical potential can be drawn with confidence as the chemical shifts are not affected by the presence of electrolyte. MK-2's ($Q/Q^{\bullet -}$) and first electrochemical potential is the one electron reduction of the quinone to semiquinone the second is the one electron reduction of the semiquinone to the dianion ($Q^{\bullet -}/Q^{2-}$), Scheme 2.[29-31] The CVs of MK-2 in each solvent are shown in Fig. 12. The Fc^{+}/Fc couple $E_{1/2}$ is set to zero as all potentials were referenced to the internal standard. The $Q/Q^{\bullet -}$ peak current is larger than that of the $Q^{\bullet -}/Q^{2-}$, which has been attributed to the repulsion of the semiquinone

Table 1. Averaged half-wave potentials of MK-2 in different solvents The $E_{1/2}$ potential measurements were done in triplicate. A Student's *t* test analysis determined that the $E_{1/2}$ of $Q/Q^{\bullet-}$ and $Q^{\bullet-}/Q^{2-}$ are statistically different in each solvent. All comparisons were at the 99.9% confidence interval (CI) at four degrees of freedom except the $Q^{\bullet-}/Q^{2-}$ CH_3CN vs. DMSO which was 98%.

Solvent	$Q/Q^{\bullet-}$ $E_{1/2}$ *vs.* Fc^+/Fc (V)	$Q^{\bullet-}/Q^{2-}$ $E_{1/2}$ *vs.* Fc^+/Fc (V)
CH_3CN	-1.230 ± 0.003	-1.902 ± 0.012
DMSO	-1.155 ± 0.001	-1.863 ± 0.008
Pyridine	-1.331 ± 0.001	-2.075 ± 0.003

from the diffusion layer of the working electrode.[42] The lower concentration of semiquinone at the electrode surface results in lower current produced, is evident by the Nernstian equation. The half-wave ($E_{1/2}$) potentials of each redox process were calculated using eq. 2 where E_{pc} and E_{pa} are the cathodic and anodic peak potentials, respectively, and are listed in Table 1. The reference Fc^+/Fc $E_{1/2}$ was subtracted from each measurement's calculated $E_{1/2}$ and then the $E_{1/2}$ *vs* Fc^+/Fc was averaged for each solvent and redox process for the triplicate measurements. The i_{pc}/i_{pa} of each half-wave potential measured was close to unity indicating reversibility or semi-reversibility. Using equation 3, the number of electrons transferred were determined to be one for each electrochemical process.

There can be various problems associated with the electrochemical measurements of quinones in organic solvents that can influence the half-wave potential observed. The major issues that are negligible for our system include: inter- and intra-molecular hydrogen bonding from solvent or hydroxyl groups on the quinone, ion-pair formation from Lewis acid cations of the electrolyte or from pyridinium ions, the working electrode adhesion of hydroquinone (QH), and from interactions of MK-2 with the internal standard.[29-31, 42-49] The water or acidic proton content greatly impacts the electrochemical potential of the semiquinone $Q^{\bullet-}/Q^{2-}$ process, while the quinone $Q/Q^{\bullet-}$ process is unaffected.[29-31, 42, 47] As the solvent's water or acidic proton

concentration increases, the concentration of hydroquinone increases. This shifts the observed semiquinone half-wave potential to more positive potentials until only one two electron wave is observed.[30-31, 42, 47] Therefore, the greater standard deviations in the $Q^{\bullet -}/Q^{2-}$ half-wave potentials are consistent with the inherent water in the solvent even after distillation and drying over activated molecular sieves.

The values determined for MK-2 in each solvent agree with literature values of substituted 1,4-napthoquinone. The literature values for the 1,4-napthoquinone in DMSO, CH_3CN, and pyridine are $Q/ Q^{\bullet -}$ $E_{1/2}$ vs Fc^+/Fc of -1.06V, -1.08V, and -1.19 V, respectively.[46] The addition of a methyl substituent lowers the $Q/ Q^{\bullet -}$ $E_{1/2}$ by approximately 70 mV while the addition of an isoprenyl unit lowers it by an additional 50-60 mV.[29] Therefore the $Q/ Q^{\bullet -}$ $E_{1/2}$ vs Fc^+/Fc for MK-2 in DMSO, CH_3CN, and pyridine, should be near -1.16 V, -1.20 V, and -1.31 V, respectively.[29, 46] The experimentally determined values for MK-2 $Q/ Q^{\bullet -}$ $E_{1/2}$ were consistent with this analysis, see Table 1.[29, 46] In Fig. 13, pg. 38 the half-wave potentials are plotted showing the trend that the $Q/ Q^{\bullet -}$ reduction is easier in DMSO than CH_3CN or pyridine. This trend is also observed in the 1,4-napthoquinone potentials for the $Q/ Q^{\bullet -}$ process in the three solvents.[46] In dimethylformamide (DMF), the $Q/ Q^{\bullet -}$ $E_{1/2}$ vs Fc^+/Fc of MK-2 was determined to be -1.233 V, close to the value for CH_3CN.[29] While the $Q^{\bullet -}/Q^{2-}$ process was not observed in DMF, the $E_{1/2}$ vs Fc^+/Fc was estimated near -1.954 V, agreeing with our values, Table 1.[29]

In summary, our measurements are in agreement with the available but incomplete data in the literature and with the predicted value of the $E_{1/2}$ for the process of $Q/Q^{\bullet -}$ for MK-2 in CH_3CN. The half-wave potentials show that the $Q/ Q^{\bullet -}$ reduction is easier in DMSO than CH_3CN or pyridine whereas there is little difference in the observed second reduction.

BIOLOGICAL IMPLICATIONS

MK-9 is a natural substrate containing a naphthoquinone and an isoprenyl side-chain with nine isoprene units that carry out the electron transfer in *Mycobacterium tuberculosis*.[3, 6] We carried out the studies described in this above to begin to understand the chemical and physical properties of MKs. We are investigating MK-2 first, because it provides us with the base structure containing the naphthoquinone unit and the isoprene side-chain. MK-2 is also easy to obtain because the precursors are inexpensive and the synthesis is relatively simple. This allows for preparation of enough material that we can conduct detailed characterization of the molecule.

The studies with MK-2 represent the first investigation of the conformation of MK and MK derivatives that are generally depicted as "Q" in textbooks and in the general literature overall.[8-9] This study was developed to investigate three hypotheses, the first involved establishing that *MKs will have different conformations depending on the specific environmental conditions.* This hypothesis was investigated by first synthesizing MK-2. Then by characterizing MK-2 conformational behavior in different organic solutions by using NMR spectroscopy. We found that different conformations are observed in DMSO, benzene and RMs; thus confirming this hypothesis.

The straight chain conformations of long chain biological molecules like fatty acids are generally drawn by life-scientists. However, a few studies show the straight chain conformations compare in energy with folded helical conformations.[50-51] Although the folded conformations may be slightly higher in energies, the difference is surprisingly small. The work that de Sousa's group does shows where the C-C bond lengths in stearic acid decrease under

high pressure. These bond shrinkages cause conformational and symmetry changes in stearic acid favoring folded conformations.[13] Studies previously carried out by Mui and Gundersen using high temperature UV-absorption spectroscopy, molecular orbital calculations and gas-phase electron diffraction found that isoprene and chloroprene conformations did, in fact, change favoring folding.[52-53] These studies are consistent with previous work carried out with fatty acids where the experimental studies showed that the conformations of these fatty acids can and do change just like MK-2 shown in this work.

The second hypothesis involved *determining if the association of MK with the membrane will influence the conformation of the MK derivative.* This question was investigated combining NMR studies of MK-2 in organic solution with NMR studies in model membrane systems and in Langmuir monolayers. The conformation of MK-2 was characterized in organic solvents and this geometry was found to differ slightly from the conformation of MK-2 when it was associated with the AOT/RM. It is to be expected that MK-2 would have an affinity for the membrane because of its hydrophobicity, and that is indeed observed both in the RM system and the Langmuir monolayer. The fact that MK-2 interacts with the monolayer is consistent with the MK affinity for the cell membrane, and the conformations found in this work are consistent with the MK-2 fold over even upon interactions with the interface. However, the conformation of MK-2 in benzene and DMSO differs slightly when MK-2 interacts with the AOT/RM interface.

The redox potentials of MK-2 depicted in Fig. 13 illustrate trends that are in agreement with published literature.[29, 46] Specifically, during the first electrochemical process producing the semiquinone, MK-2 has the most positive potential in DMSO and the most negative

potential in pyridine, showing it is easier to reduce MK-2 in DMSO than pyridine. This would align with the folded molecular model where the conformation in DMSO (60.5 kJ/mol) is slightly lower in energy than in benzene (60.9 kJ/mol). This result combined with other conformational changes observed in addition to the differing redox potentials between solvents support this hypothesis. Therefore the hypothesis is supported that the redox potential can be associated with the conformation of the MK-2.

Depending on solvent environment, the isoprene chain molecular orbitals interact differently with those of the naphthoquinone. This leads to conformations of varying energy which can be directly correlated to the energy required to reduce the naphthoquinone. The energy required for the reduction is determined by the energy of the lowest unoccupied molecular orbital (LUMO) that the electrons occupy.[54] Differences in how the isoprene chain folds in the different solvents will influence these molecular orbitals, resulting in energy differences of the available LUMO to accept the electron. This aligns with our third hypothesis, *that the structure or conformation of MK-2 in each solvent and its redox potential are correlated*.

Characterization of MK-2 is only part of the investigations needed to fully understand the natural substrate MK-9, the MK derivative used in *Mycobacterium tuberculosis.* MK-2 is shorter than the other biologically relevant MK structures with MK-4 (vitamin K_2) and MK-9 (MK used in MenJ) being the most well-known examples. Since MK-2's isoprene chain is shorter than MK-4 and MK-9, it may not fully undergo interactions found by the longer isoprene chains. The results show that the folding of MK-2 is very important, and the results suggest that the MK derivatives with the longer

chain will fold as well. However, understanding how these compounds fold in a hydrophobic environment is important understanding how they will function in the membrane.

CONCLUSION

MK-9 is an important part of the electron transfer process in *Mycobacterium tuberculosis.*[3, 6] The studies described in this work help us to begin to understand the chemical and physical properties of MKs. Using a small model system, MK-2, as a representative MK derivative and we find that in contrast to the extended conformation generally depicted in life science text books that MK-2 is in a folded conformation.

The electrochemistry, NMR spectroscopy and molecular modeling, allows us to conclude that MK-2's conformation is solvent dependent and that we can confirm this by their electrochemical potentials being statistically different in the solvents and environments tested. This finding is important for the implication that similar results will be obtained with other MK derivatives. Ultimately, the biological implications for the characterization of MK-2 relates to the details of the interaction of MK-9 with the electron transfer complex in *Mycobacterium tuberculosis.*

FIGURES

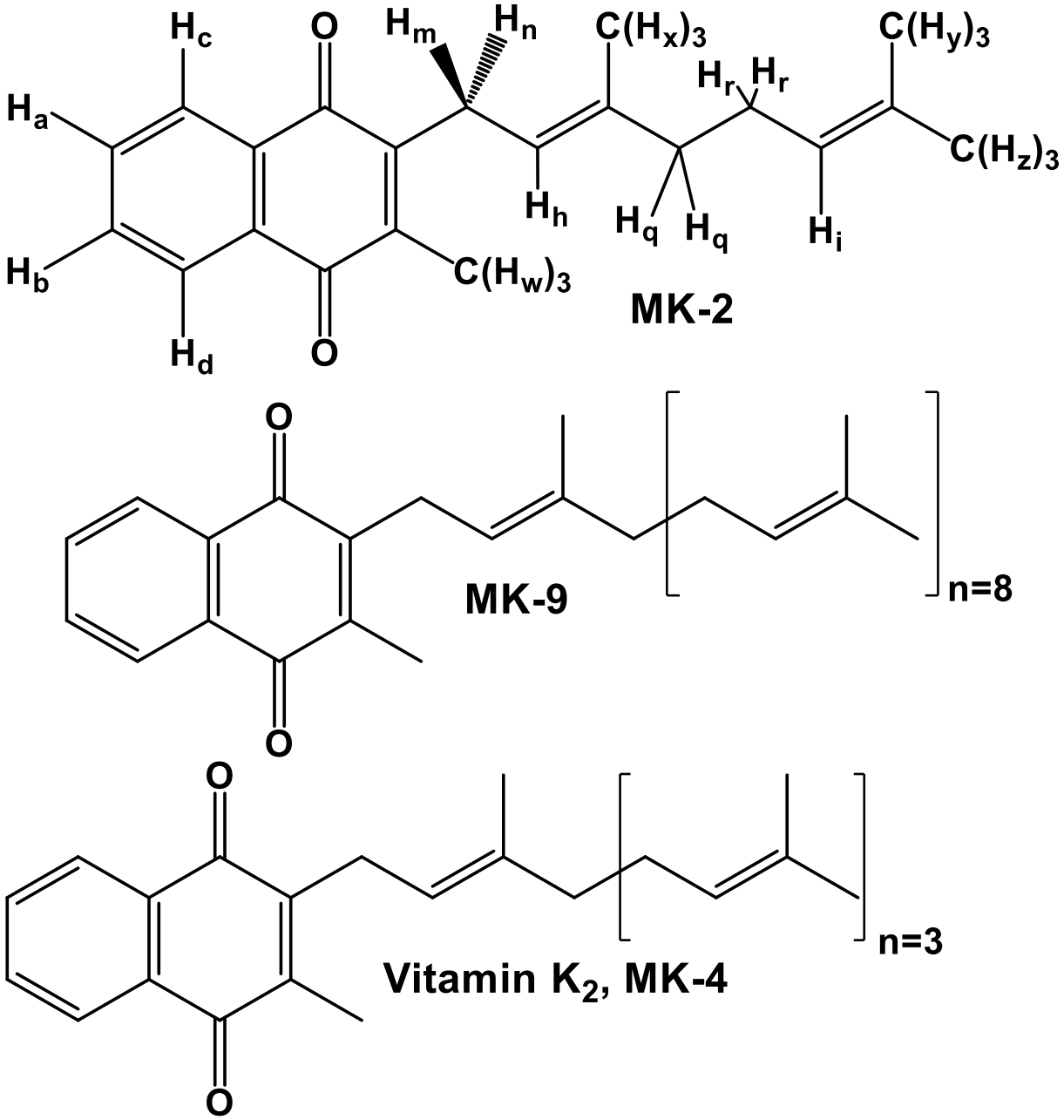

Fig. 1. Biologically relevant MK derivatives (MK-9 and MK-4) and MK-2. MK-4 in humans is better known as vitamin K_2 and MK-9 is found in *Mycobacterium tuberculosis*

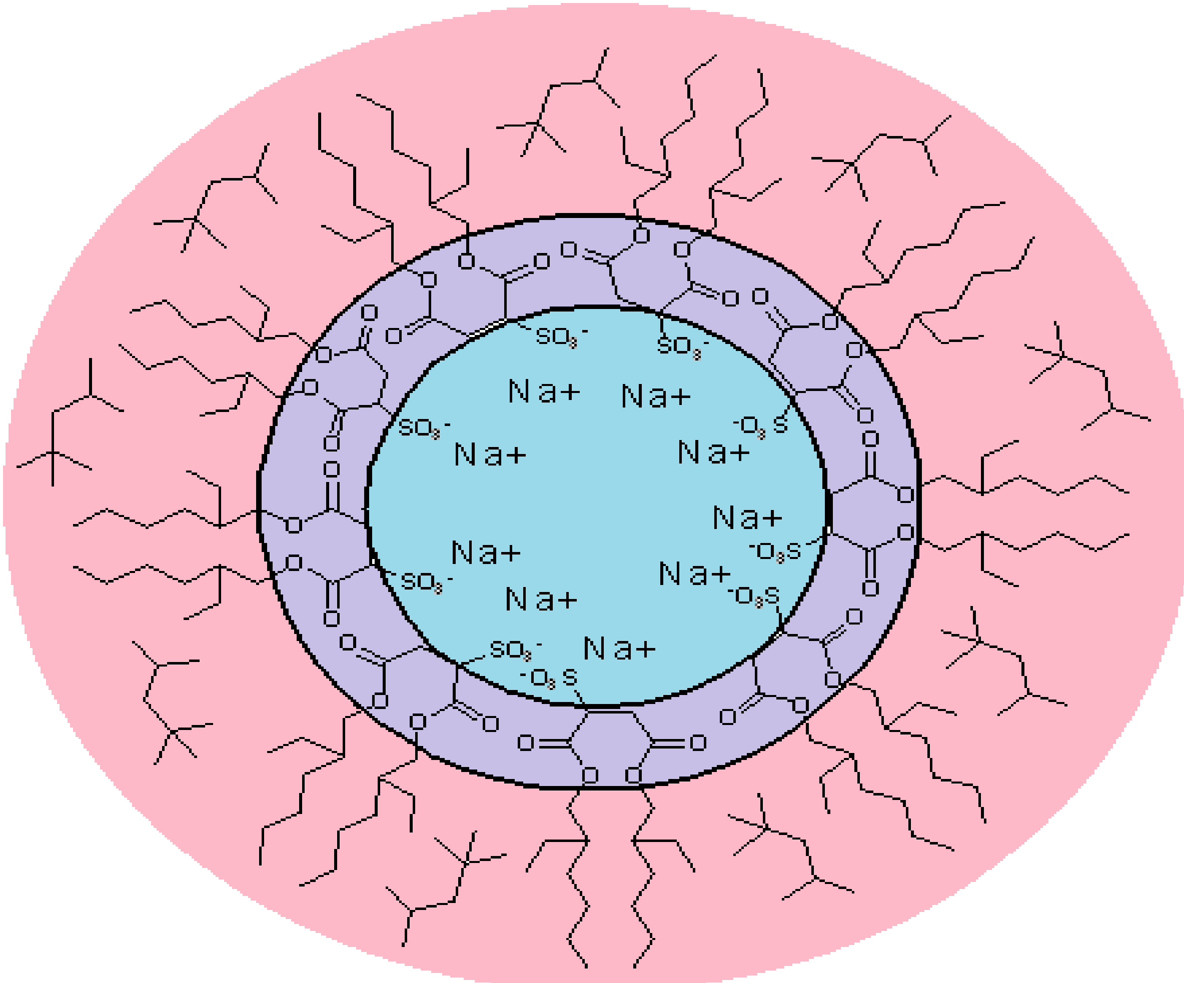

Fig. 2. Schematic diagram of a reverse micelle present in a microemulsion. The water pool (blue), The Stern layer (purple), the surfactant tails (pink), and the organic solvent (isooctane; pink and white space outside the pink).

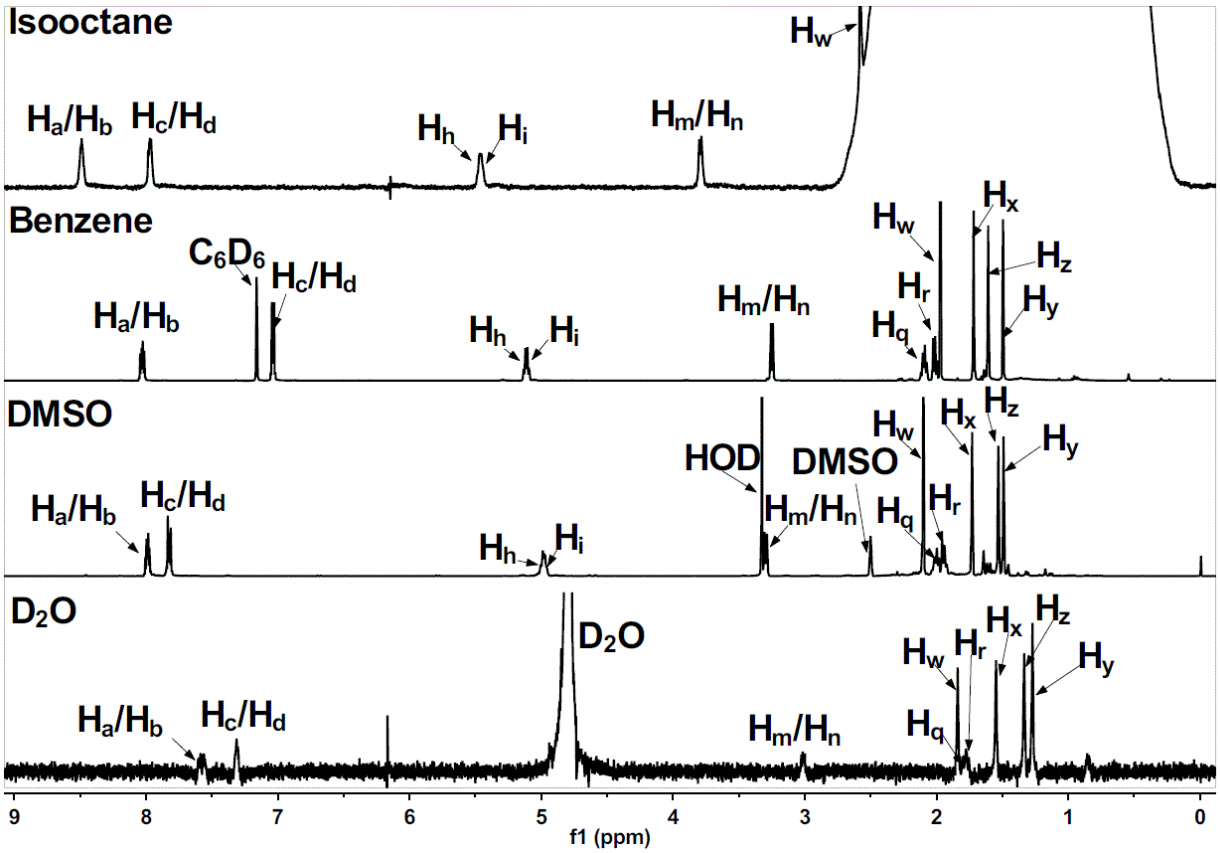

Fig. 3. Stacked 1D ^{1}H NMR spectra of MK-2 in hydrophilic (D_2O and DMSO) and hydrophobic (benzene and isooctane) solvents. Peak labeling corresponds to MK-2 structure in Fig. 1.

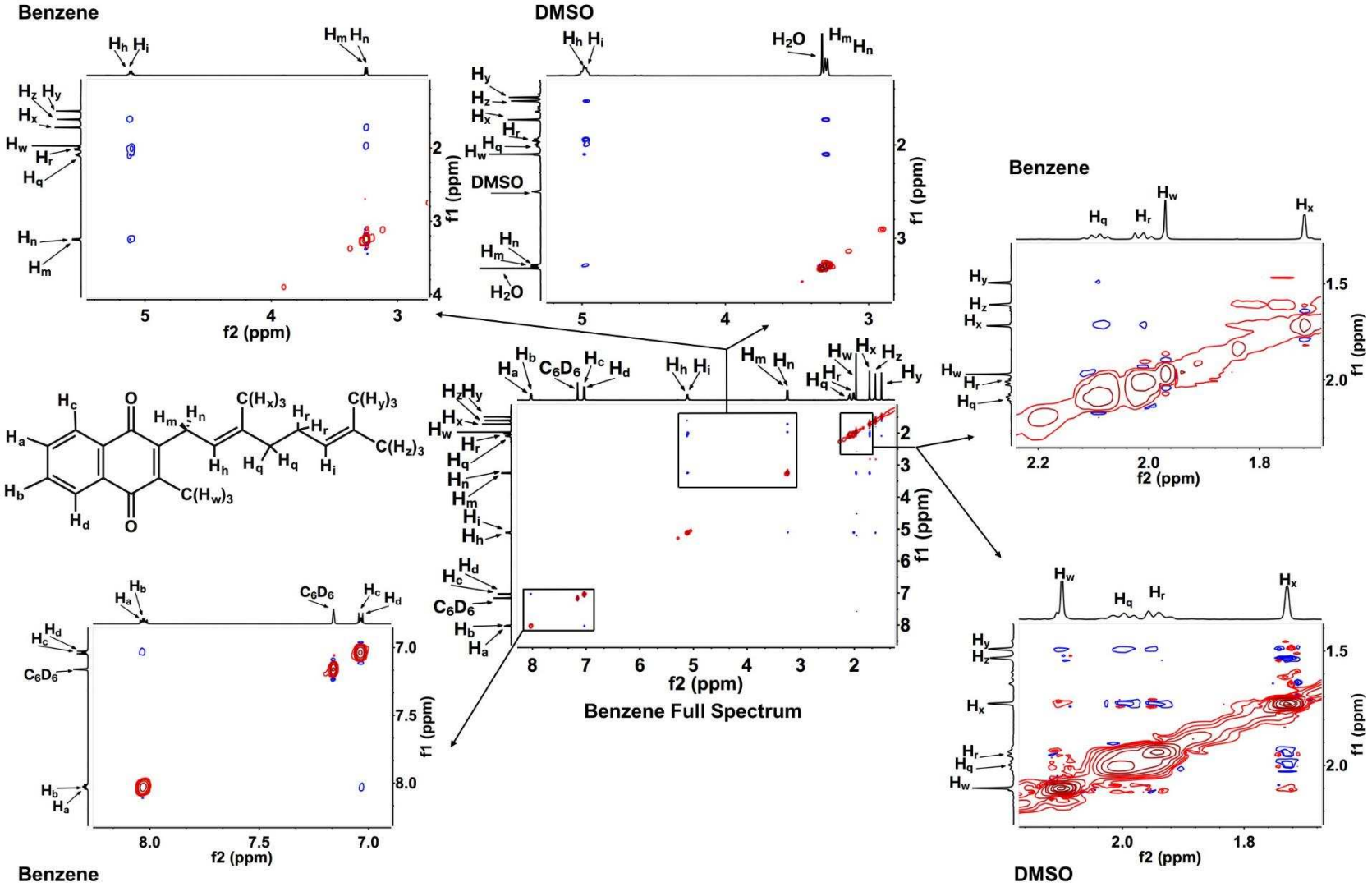

Fig. 4. ^{1}H-^{1}H 2D NOSEY spectra of MK-2 in benzene and DMSO. The figure in the center is the full spectrum of MK-2 in benzene, while the outer spectra are selected regions of full spectrum enlarged in benzene and DMSO.

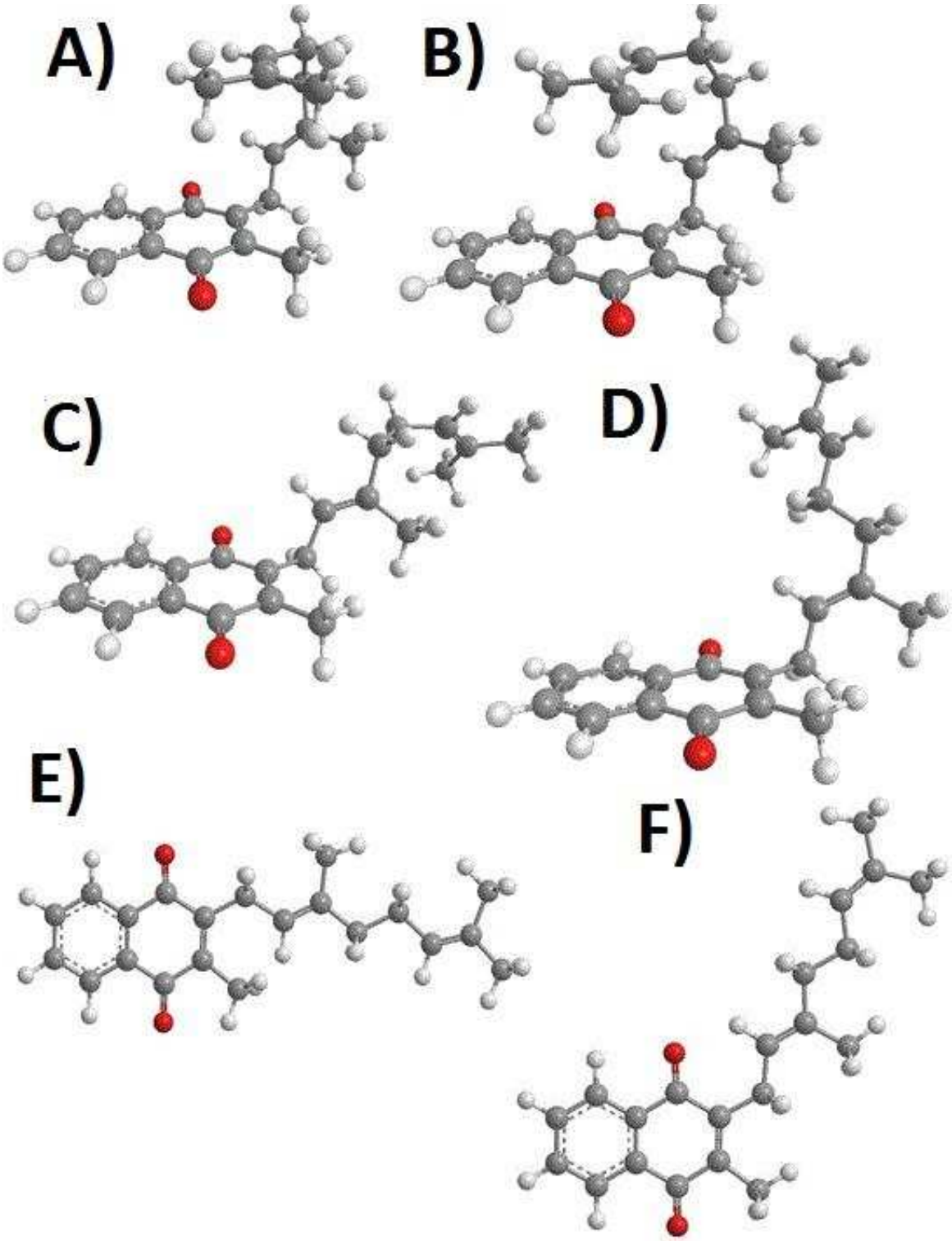

Fig. 5. MK-2 Conformations generated with MMFF94 calculations in the gas phase. A) DMSO: 60.5 kJ/mol, H_w-H_y: 2.60 Å, B) benzene: 60.9 kJ/mol, H_w-H_y: 3.60 Å, C) a low energy structure: 63.3 kJ/mol, H_w-H_y: 6.60 Å, D) a structure resembling the commonly drawn conformation - elongated tail out of quinone plane with energy minimization: 63.5 kJ/mol, H_w-H_y: 7.80 Å, E) commonly drawn: w/o energy minimization: 124 kJ/mol, H_w-H_y: 7.90 Å, F) commonly drawn: elongated tail: 83.1 kJ/mol, H_w-H_y: 8.90 Å.

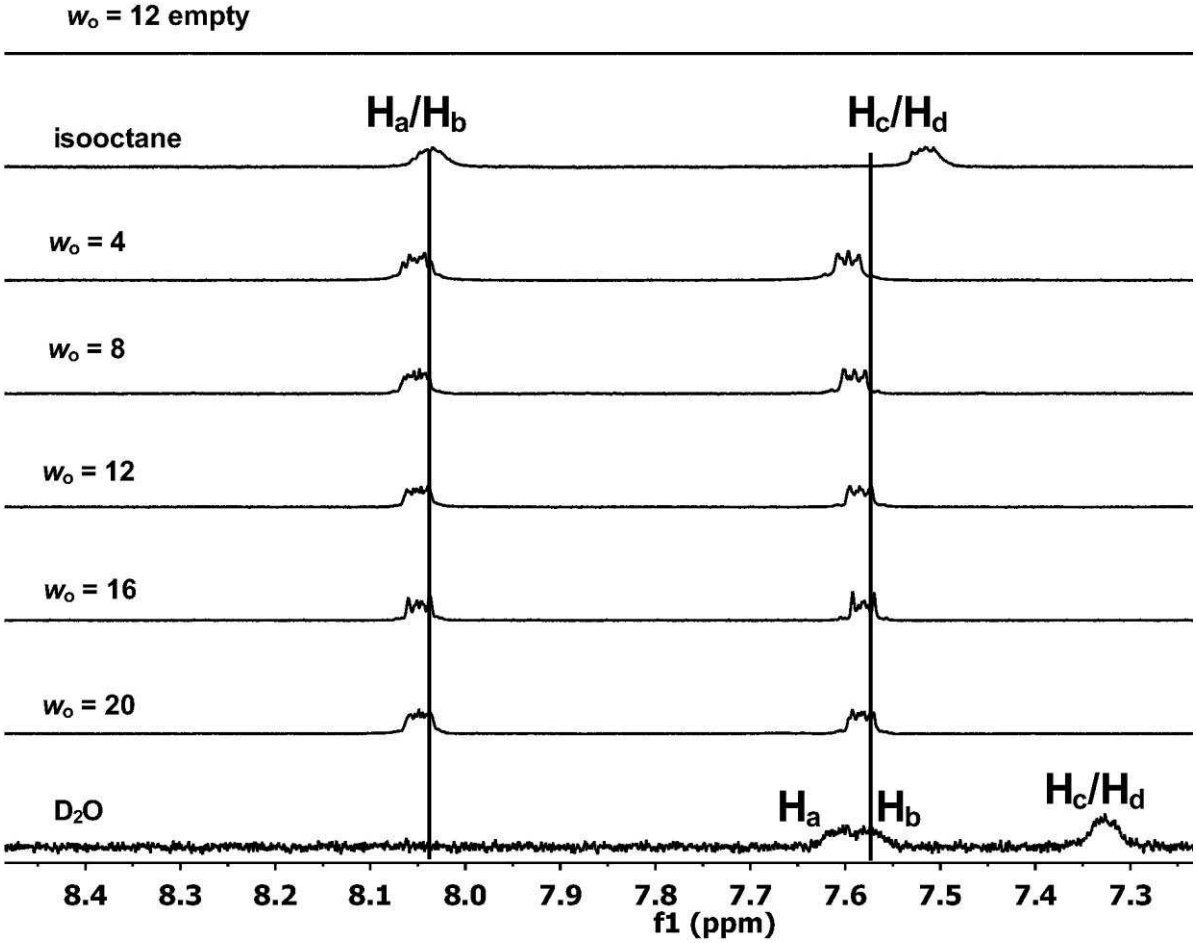

Fig. 6. 1D ^{1}H NMR spectra of MK-2's aromatic protons, H_a, H_b, H_c, and H_d in D_2O, isooctane and different sized reverse micelles. Peaks labeled with corresponding protons MK-2 (see Fig. 1). H_a, H_b, H_c, and H_d protons undergo a shift upon inclusion in RMs.

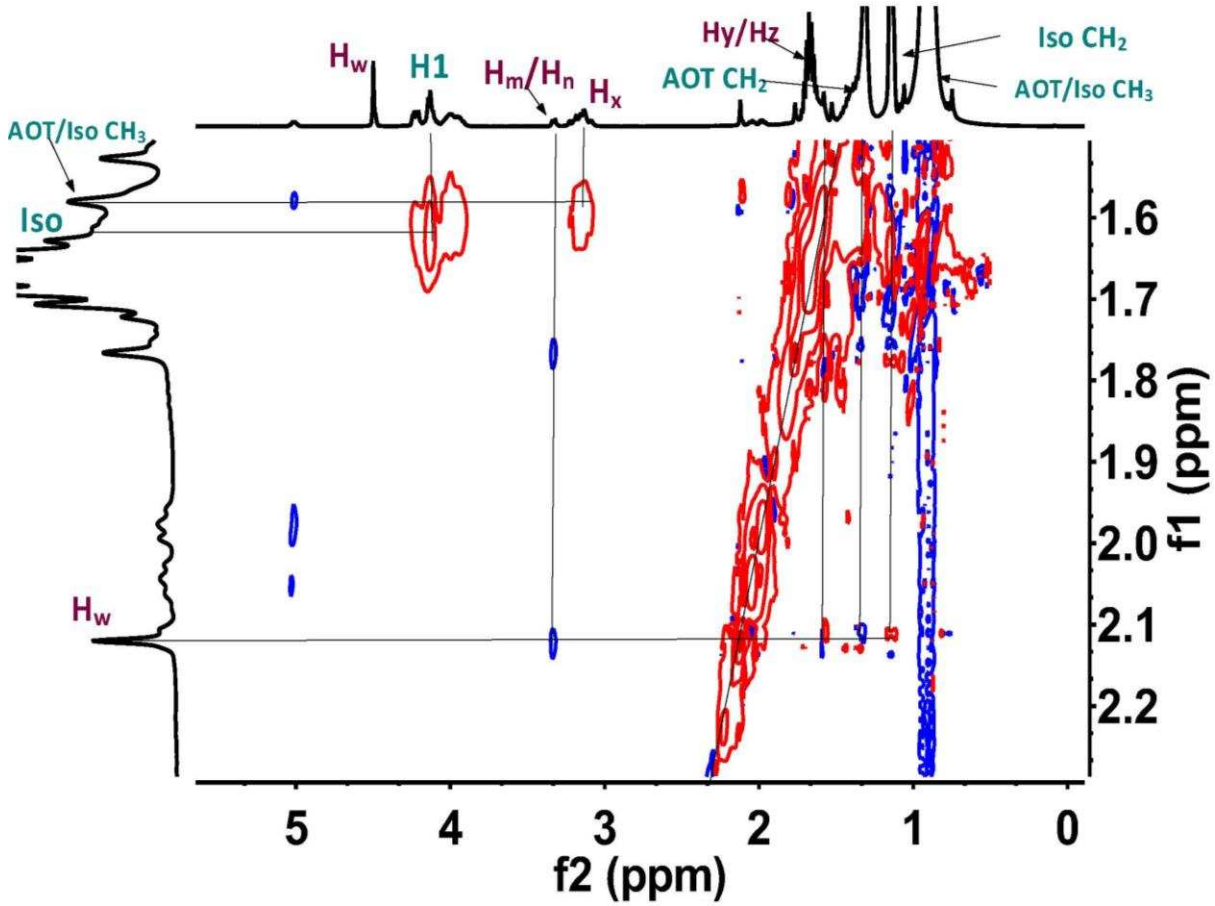

Fig. 7. The partial ^{1}H-^{1}H 2D NOESY NMR spectrum showing how the MK-2 conformation folds within the RM interface. The plum color show MK-2 to MK-2 interactions, teal shows AOT to AOT interactions and plum to teal shows MK-2 to AOT interactions.

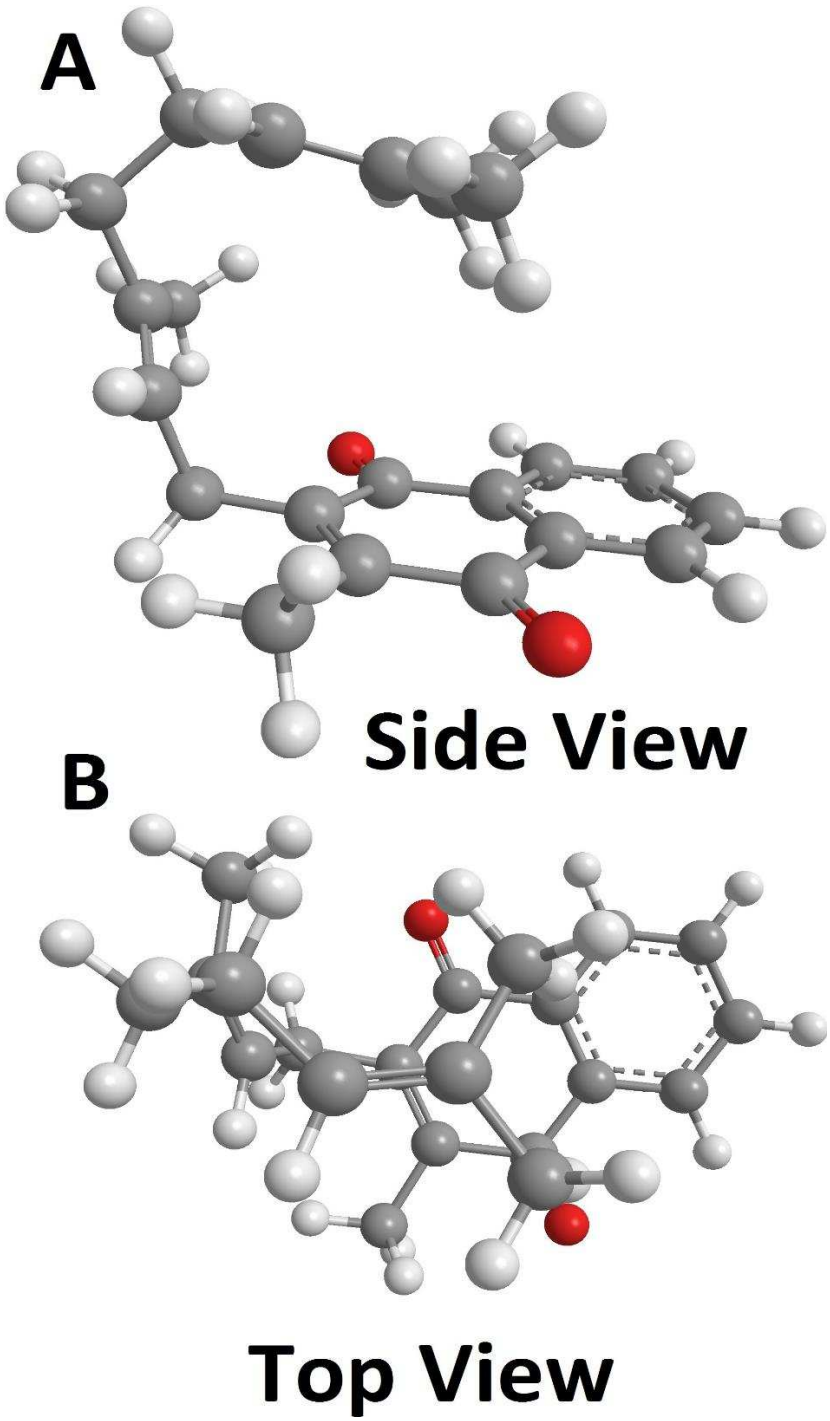

Fig. 8. MMFF94 molecular dynamics simulations generating the 3D conformation of MK-2 in a RM that is consistent with ^{1}H-^{1}H 2D NOESY NMR spectra. a) Side view of minimized conformation (60.5 kJ/mol) showing that MK-2's isoprene chain adopting a hook-like shape. B) Top view of minimized conformation showing the terminal isoprene methyl-groups overlapping the carbonyl groups.

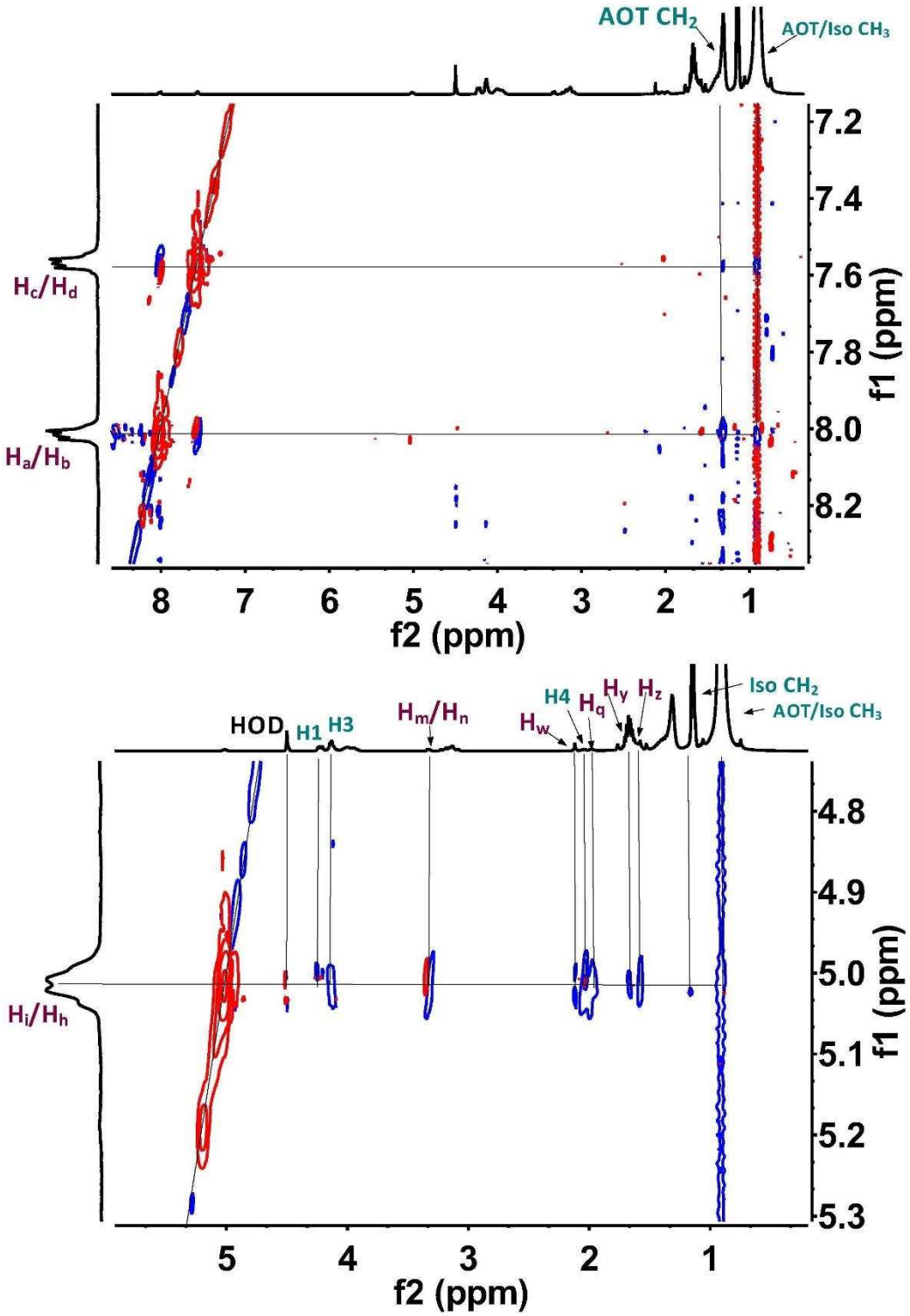

Fig. 9. ^{1}H-^{1}H 2D NOESY NMR showing were MK-2 sits within the AOT surfactant tails. The plum color shows MK-2 to MK-2 interactions, teal shows AOT to AOT interactions and plum to teal shows MK-2 to AOT interactions. A) Interactions between MK-2's aromatic protons and AOT. B) Interactions between other MK-2 protons and AOT.

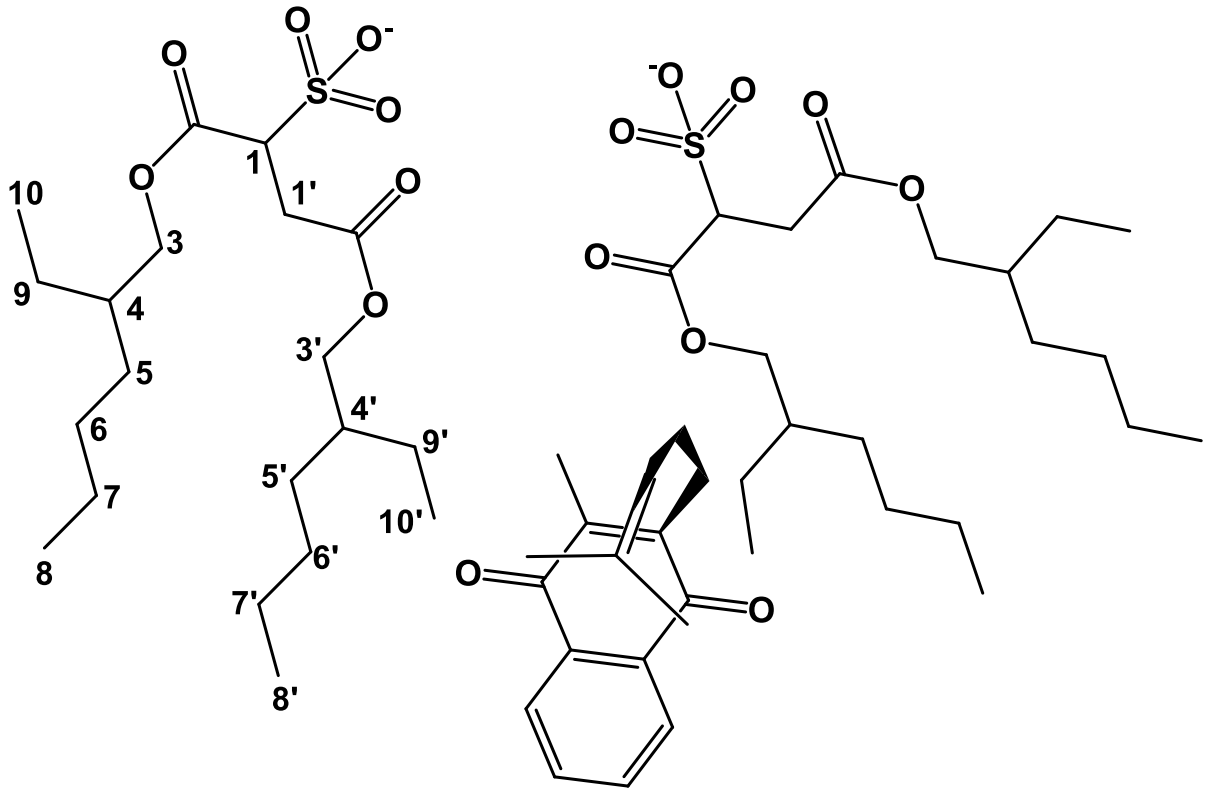

Fig. 10. Schematic cartoon of MK-2's folded conformation and placement in the RM interface. This arrangement is consistent with ^{1}H-^{1}H NOESY NMR. Some bonds in MK-2's isoprene chain were omitted for clarity.

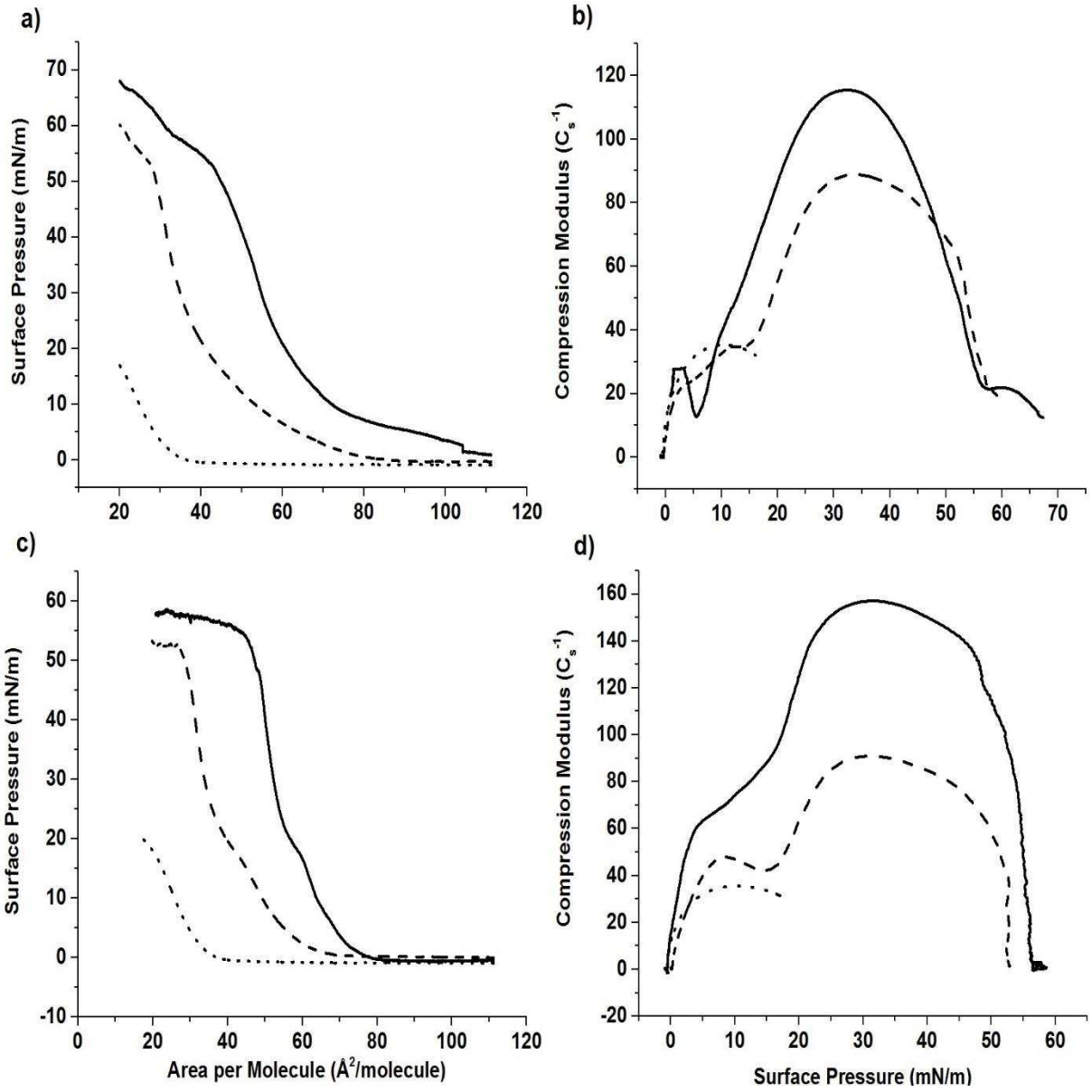

Fig. 11. Compression isotherms of MK-2 films (dotted lines), DPPC or DPPE (solid lines), or a 50:50 mixture of MK-2 and lipid (dashed line). Each graph represents the compression isotherms of MK-2 and DPPC (a), the resulting compression modulus (b), the compression isotherm of MK-2 and DPPE, and the resulting compression modulus (d).

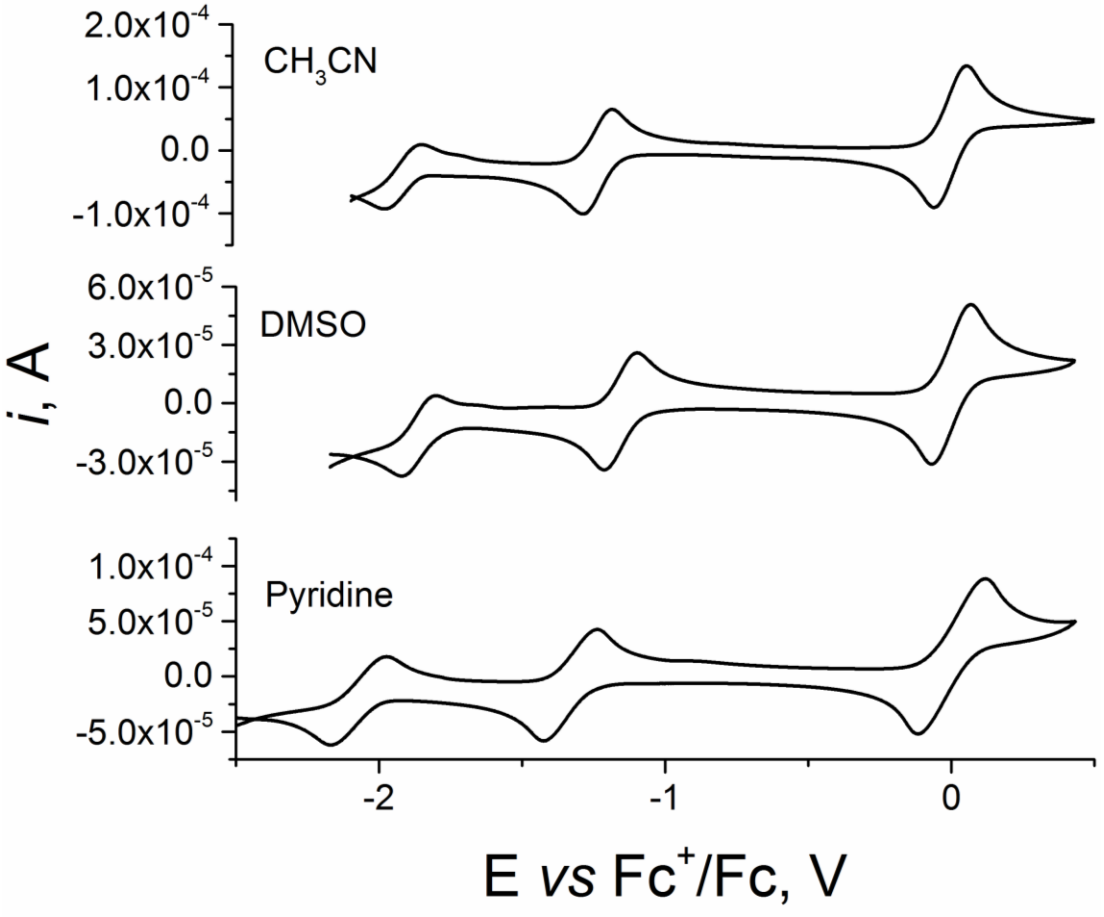

Fig. 12. Cyclic voltammograms of 2 mM MK-2 in CH_3CN, DMSO, and pyridine. The potentials are referenced to the Fc^+/Fc couple (2 mM) determined in each solvent. Each sample has 0.1 M TBAP and was degassed with Ar (g) for 10 minutes at ambient room temperature before spectra were recorded.

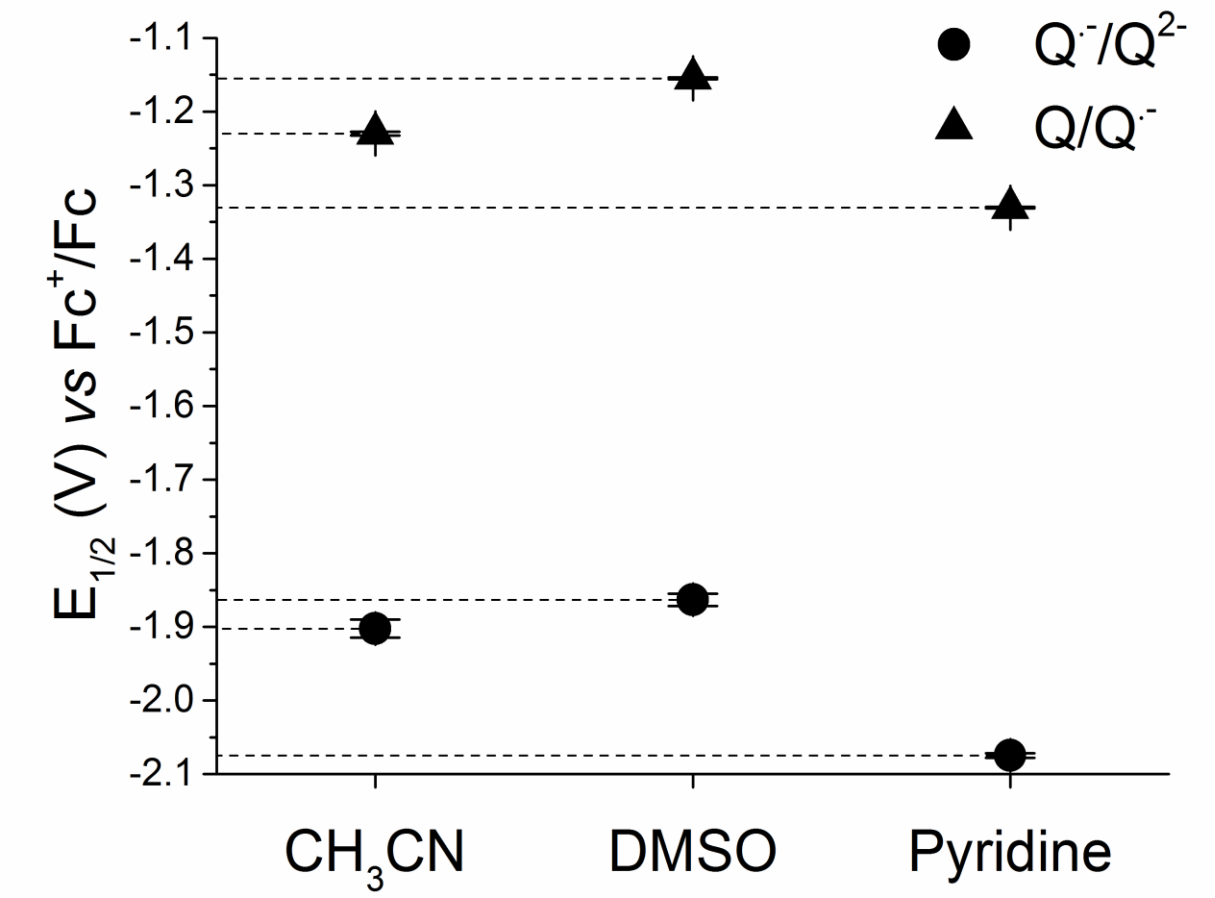

Fig. 13. Determined $E_{1/2}$ (*vs* Fc^+/Fc in V) of MK-2 $Q/Q^{\bullet-}$ and $Q^{\bullet-}/Q^{2-}$ redox processes versus solvent. Added lines show the distinction between each solvent for each redox process. Each solvent was run in triplicate, with error bars shown. Student's *t* test indicated the half wave potentials of each redox process are significantly different in each solvent, (98% CI for $Q^{\bullet-}/Q^{2-}$ CH_3CN-DMSO, 99.9% CI for all other comparisons).

REFERENCES

1. da Costa, M. S.; Albuquerque, L.; Nobre, M. F.; Wait, R., The Extraction and Identification of Respiratory Lipoquinones of Prokaryotes and Their Use in Taxonomy. In *Methods in Microbiology, Vol 38: Taxonomy of Prokaryotes*, Rainey, F.; Oren, A., Eds. Elsevier Academic Press Inc: San Diego, 2011; Vol. 38, pp 197-206.
2. Kroppenstedt, R. M.; Mannheim, W., LIPOQUINONES IN MEMBERS OF THE FAMILY PASTEURELLACEAE. *Int. J. Syst. Bacteriol.* **1989,** *39* (3), 304-308.
3. Collins, M. D.; Jones, D., DISTRIBUTION OF ISOPRENOID QUINONE STRUCTURAL TYPES IN BACTERIA AND THEIR TAXONOMIC IMPLICATIONS. *Microbiol. Rev.* **1981,** *45* (2), 316-354.
4. Meganathan, R., Biosynthesis of menaquinone (vitamin K2) and ubiquinone (coenzyme Q): A perspective on enzymatic mechanisms. In *Vitamins & Hormones*, Academic Press: 2001; Vol. Volume 61, pp 173-218.
5. Upadhyay, A.; Fontes, F. L.; Gonzalez-Juarrero, M.; McNeil, M. R.; Crans, D. C.; Jackson, M.; Crick, D. C., Partial Saturation of Menaquinone in Mycobacterium tuberculosis: Function and Essentiality of a Novel Reductase, MenJ. *Acs Central Science* **2015,** *1* (6), 292-302.
6. Collins, M. D.; Kroppenstedt, R. M., STRUCTURES OF THE PARTIALLY SATURATED MENAQUINONES OF GLYCOMYCES-RUTGERSENSIS. *FEMS Microbiol. Lett.* **1987,** *44* (2), 215-219.
7. Bentley, R., BIOSYNTHESIS OF VITAMIN-K AND OTHER NATURAL NAPHTHOQUINONES. *Pure Appl. Chem.* **1975,** *41* (1-2), 47-68.
8. Cooper, G. M.; Hausman, R. E., *The Cell A Molecular Approach*. 5th ed.; Sinauer Associates, INC.: Sunderland, Massachusetts, USA, 2009; p 820.
9. Nelson, D. L.; Cox, M. M., *Lehninger Principles of Biochemistry*. 5th ed.; W.H. Freeman and Company: New York, USA, 2008; p 1158.
10. Lowry, T. H.; Richardson, K. S., *Mechanism and Theory in Organic Chemistry*. 3rd ed.; Harper & Row, Publishers New York, USA, 1987; p 1090.
11. Sedov, I. A.; Solomonov, B. N., Relation between the characteristic molecular volume and hydrophobicity of nonpolar molecules. *J. Chem. Thermodyn.* **2010,** *42* (9), 1126-1130.
12. Law, J. M. S.; Setiadi, D. H.; Chass, G. A.; Csizmadia, I. G.; Viskolcz, B., Flexibility of "polyunsaturated fatty acid chains" and peptide backbones: A comparative ab initio study. *Journal of Physical Chemistry A* **2005,** *109* (3), 520-533.
13. de Sousa, F. F.; Freire, P. T. C.; Saraiva, G. D.; Lima, J. A.; Alcantara, P.; Melo, F. E. A.; Mendes, J., Pressure-induced phase transitions in stearic acid C form. *Vibrational Spectroscopy* **2010,** *54* (2), 118-122.
14. Sostarecz, A. G.; Gaidamauskas, E.; Distin, S.; Bonetti, S. J.; Levinger, N. E.; Crans, D. C., Correlation of Insulin-Enhancing Properties of Vanadium-Dipicolinate Complexes in Model Membrane Systems: Phospholipid Langmuir Monolayers and AOT Reverse Micelles. *Chemistry-a European Journal* **2014,** *20* (17), 5149-5159.
15. Riter, R. E.; Kimmel, J. R.; Undiks, E. P.; Levinger, N. E., Novel reverse micelles partitioning nonaqueous polar solvents in a hydrocarbon continuous phase. *J. Phys. Chem. B* **1997,** *101* (41), 8292-8297.

16. Maitra, A., DETERMINATION OF SIZE PARAMETERS OF WATER AEROSOL OT OIL REVERSE MICELLES FROM THEIR NUCLEAR MAGNETIC-RESONANCE DATA. *Journal of Physical Chemistry* **1984,** *88* (21), 5122-5125.
17. Durantini, A. M.; Falcone, R. D.; Silber, J. J.; Correa, N. M., Effect of Confinement on the Properties of Sequestered Mixed Polar Solvents: Enzymatic Catalysis in Nonaqueous 1,4-Bis-2-ethylhexylsulfosuccinate Reverse Micelles. *ChemPhysChem* **2016,** *17* (11), 1678-1685.
18. Lepori, C. M. O.; Correa, N. M.; Silber, J. J.; Falcone, R. D., How the cation 1-butyl-3-methylimidazolium impacts the interaction between the entrapped water and the reverse micelle interface created with an ionic liquid-like surfactant. *Soft Matter* **2016,** *12* (3), 830-844.
19. Sedgwick, M. A.; Trujillo, A. M.; Hendricks, N.; Levinger, N. E.; Crans, D. C., Coexisting Aggregates in Mixed Aerosol OT and Cholesterol Microemulsions. *Langmuir* **2011,** *27* (3), 948-954.
20. Zan, G. T.; Wu, Q. S., Biomimetic and Bioinspired Synthesis of Nanomaterials/Nanostructures. *Adv. Mater.* **2016,** *28* (11), 2099-2147.
21. Odella, E.; Falcone, R. D.; Silber, J. J.; Correa, N. M., Nanoscale Control Over Interfacial Properties in Mixed Reverse Micelles Formulated by Using Sodium 1,4-bis-2-ethylhexylsulfosuccinate and Tri-n-octyl Phosphine Oxide Surfactants. *ChemPhysChem* **2016,** *17* (15), 2407-2414.
22. Kuchler, A.; Yoshimoto, M.; Luginbuhl, S.; Mavelli, F.; Walde, P., Enzymatic reactions in confined environments. *Nat. Nanotechnol.* **2016,** *11* (5), 409-420.
23. Dharaiya, N.; Bahadur, P., Phenol induced growth in Triton X-100 micelles: Effect of pH and phenols' hydrophobicity. *Colloid Surf. A-Physicochem. Eng. Asp.* **2012,** *410*, 81-90.
24. Dumas, C.; Meledandri, C. J., Insights into the Partitioning Behavior of Secondary Surfactants in a Microemulsion-Based Synthesis of Metal Nanoparticles: A DLS and 2D NMR Spectroscopic Investigation. *Langmuir* **2015,** *31* (26), 7193-7203.
25. Kaur, G.; Chiappisi, L.; Prevost, S.; Schweins, R.; Gradzielski, M.; Mehta, S. K., Probing the Microstructure of Nonionic Microemulsions with Ethyl Oleate by Viscosity, ROESY, DLS, SANS, and Cyclic Voltammetry. *Langmuir* **2012,** *28* (29), 10640-10652.
26. Peters, B. J.; Groninger, A. S.; Fontes, F. L.; Crick, D. C.; Crans, D. C., Differences in Interactions of Benzoic Acid and Benzoate with Interfaces. *Langmuir* **2016,** *32* (37), 9451-9459.
27. Lancaster, C. R. D.; Haas, A. H.; Madej, M. G.; Mileni, M., Recent progress on obtaining theoretical and experimental support for the "E-pathway hypothesis" of coupled transmembrane electron and proton transfer in dihaem-containing quinol : fumarate reductase. *Biochimica Et Biophysica Acta-Bioenergetics* **2006,** *1757* (8), 988-995.
28. Roura-Perez, G.; Quiroz, B.; Aguilar-Martinez, M.; Frontana, C.; Solano, A.; Gonzalez, I.; Bautista-Martinez, J. A.; Jimenez-Barbero, J.; Cuevas, G., Remote position substituents as modulators of conformational and reactive properties of quinones. Relevance of the pi/pi intramolecular interaction. *Journal of Organic Chemistry* **2007,** *72* (6), 1883-1894.
29. Prince, R. C.; Leslie Dutton, P.; Malcolm Bruce, J., Electrochemistry of ubiquinones. *FEBS Letters* **1983,** *160* (1), 273-276.
30. Guin, P. S.; Das, S.; Mandal, P. C., Electrochemical Reduction of Quinones in Different Media: A Review. *International Journal of Electrochemistry* **2011,** *2011*, 22.
31. Dryhurst, G., Kadish, K. M., Scheller, F., Renneberg, R. , *Biological Eletrochemistry*. Academic Press: New York, 1982.

32. Stahla, M. L.; Baruah, B.; James, D. M.; Johnson, M. D.; Levinger, N. E.; Crans, D. C., H-1 NMR studies of aerosol-OT reverse micelles with alkali and magnesium counterions: Preparation and analysis of MAOTs. *Langmuir* **2008,** *24* (12), 6027-6035.
33. Payne, R. J.; Daines, A. M.; Clark, B. M.; Abell, A. D., Synthesis and protein conjugation studies of vitamin K analogues. *Bioorganic & Medicinal Chemistry* **2004,** *12* (22), 5785-5791.
34. Suhara, Y.; Wada, A.; Tachibana, Y.; Watanabe, M.; Nakamura, K.; Nakagawa, K.; Okano, T., Structure-activity relationships in the conversion of vitamin K analogues into menaquinone-4. Substrates essential to the synthesis of menaquinone-4 in cultured human cell lines. *Bioorganic & Medicinal Chemistry* **2010,** *18* (9), 3116-3124.
35. Dobrinescu, C.; Iorgulescu, E. E.; Mihailciuc, C.; Macovei, D.; Wuttke, S.; Kemnitz, E.; Parvulescu, V. I.; Coman, S. M., One-Pot Hydroacetylation of Menadione (Vitamin K3) to Menadiol Diacetate (Vitamin K4) by Heterogeneous Catalysis. *Advanced Synthesis & Catalysis* **2012,** *354* (7), 1301-1306.
36. Samart, N.; Beuning, C. N.; Haller, K. J.; Rithner, C. D.; Crans, D. C., Interaction of a Biguanide Compound with Membrane Model Interface Systems: Probing the Properties of Antimalaria and Antidiabetic Compounds. *Langmuir* **2014,** *30* (29), 8697-8706.
37. A.P., G.-E.; L.J., B., Fundamental Biomedical Technologies Nanobiotechnology of Biomimetic Membranes In *Nanobiotechnology of Biomimetic Membranes*, M.K., M., Ed. Springer: New York, NY USA, 2007; pp 23-74.
38. Pirrung, M. C., *The Synthetic Chemist's Companion* John Wiley and Sons, Inc.: Hoboken, New Jersey, USA, 2007; p 198.
39. Patterson, M.; Vogel, H. J.; Prenner, E. J., Biophysical characterization of monofilm model systems composed of selected tear film phospholipids. *Biochimica Et Biophysica Acta-Biomembranes* **2016,** *1858* (2), 403-414.
40. Wang, Z. N.; Yang, S. H., Effects of Fullerenes on Phospholipid Membranes: A Langmuir Monolayer Study. *ChemPhysChem* **2009,** *10* (13), 2284-2289.
41. Luder, W. F.; Kraus, P. B.; Kraus, C. A.; Fuoss, R. M., Properties of Electrolytic Solutions. XVII. The Conductance of Some Salts in Benzene and Dioxane. *J. Am. Chem. Soc.* **1936,** *58* (2), 255-258.
42. Wawzonek, S.; Berkey, R.; Blaha, E. W.; Runner, M. E., Polarographic Studies in Acetonitrile and Dimethylformamide: III . Behavior of Quinones and Hydroquinones. *Journal of The Electrochemical Society* **1956,** *103* (8), 456-459.
43. Eggins, B. R., Interpretation of electrochemical reduction and oxidation waves of quinone-hydroquinone system in acetonitrile. *Journal of the Chemical Society D: Chemical Communications* **1969,** (21), 1267-1268.
44. Fujinaga, T.; Izutsu, K.; Nomura, T., Effect of metal ions on the polarographic reduction of organic compounds in dipolar arrotic solvents. *Journal of Electroanalytical Chemistry and Interfacial Electrochemistry* **1971,** *29* (1), 203-209.
45. Hart, J. P.; Shearer, M. J.; McCarthy, P. T.; Rahim, S., Voltammetric behaviour of phylloquinone (vitamin K1) at a glassy-carbon electrode and determination of the vitamin in plasma using high-performance liquid chromatography with electrochemical detection. *Analyst* **1984,** *109* (4), 477-481.

46. Jaworski, J. S.; Leniewska, E.; Kalinowski, M. K., Solvent effect on the redox potential of quinone-semiquinone systems. *Journal of Electroanalytical Chemistry and Interfacial Electrochemistry* **1979,** *105* (2), 329-334.
47. Kolthoff, I. M.; Reddy, T. B., Polarography and Voltammetry in Dimethylsulfoxide. *Journal of The Electrochemical Society* **1961,** *108* (10), 980-985.
48. Turner, W. R.; Elving, P. J., Electrochemical Behavior of the Quinone-Hydroquinone System in Pyridine. *Journal of The Electrochemical Society* **1965,** *112* (12), 1215-1217.
49. Eggins, B. R.; Chambers, J. Q., Electrochemical oxidation of hydroquinone in acetonitrile. *Journal of the Chemical Society D: Chemical Communications* **1969,** (5), 232-233.
50. Bock, C. W.; Panchenko, Y. N.; Krasnoshchiokov, S. V.; Aroca, R., ABINITIO STRUCTURES AND VIBRATIONAL ANALYSIS OF THE ISOPRENE CONFORMERS. *Journal of Molecular Structure* **1987,** *160* (3-4), 337-346.
51. Squillacote, M. E.; Semple, T. C.; Mui, P. W., THE GEOMETRIES OF THE S-CIS CONFORMERS OF SOME ACYCLIC 1,3-DIENES - PLANAR OR TWISTED. *J. Am. Chem. Soc.* **1985,** *107* (24), 6842-6846.
52. Mui, P. W.; Grunwald, E., ENTHALPY CHANGE FOR THE S-TRANS TO S-CIS CONFORMATIONAL EQUILIBRIUM IN 2-METHYL-1,3-BUTADIENE (ISOPRENE), AS STUDIED BY HIGH-TEMPERATURE ULTRAVIOLET-ABSORPTION SPECTROSCOPY. *Journal of Physical Chemistry* **1984,** *88* (25), 6340-6344.
53. Gundersen, G.; Thomassen, H. G., THE MOLECULAR-STRUCTURE AND CONFORMATIONAL BEHAVIOR OF 2-CHLORO-1,3-BUTADIENE (CHLOROPRENE) STUDIED BY GAS-PHASE ELECTRON-DIFFRACTION AND AB-INITIO MO CALCULATIONS. *Journal of Molecular Structure* **1991,** *243* (3-4), 385-409.
54. Peover, M. E., 879. A polarographic investigation into the redox behaviour of quinones: the roles of electron affinity and solvent. *Journal of the Chemical Society (Resumed)* **1962,** (0), 4540-4549.
55. Eicke, H. F.; Rehak, J., FORMATION OF WATER-OIL-MICROEMULSIONS. *Helvetica Chimica Acta* **1976,** *59* (8), 2883-2891.
56. Zulauf, M.; Eicke, H. F., INVERTED MICELLES AND MICROEMULSIONS IN THE TERNARY-SYSTEM H2O-AEROSOL-OT-ISOOCTANE AS STUDIED BY PHOTON CORRELATION SPECTROSCOPY. *Journal of Physical Chemistry* **1979,** *83* (4), 480-486.

APPENDIX

Table A1. Selected Conformation Energies of MK-2 and Selected Bond Lengths Between Protons
[a]All distances were determined using the closest protons. For example, the closest H_w proton was used to determine the distance.

MK-2 Conformation	Energy (kJ/mol)	H_w-H_m [a] (Å)	H_w-H_n[a] (Å)	H_w-H_q[a] (Å)	H_w-H_r[a] (Å)	H_w-H_y[a] (Å)	H_w-H_z [a] (Å)
DMSO	60.5	3.60	2.10	5.90	5.30	2.60	3.70
Benzene	60.9	3.60	2.10	5.80	4.90	3.60	5.90
Representative High Energy	63.3	3.70	2.20	4.60	5.90	6.60	7.60
Elongated Tail Out of Quinone Plane	63.5	3.70	2.20	4.80	5.20	7.80	9.20
Without Energy Minimization	124	3.40	3.60	3.30	5.60	7.90	7.80
With Elongated Tail	83.1	2.30	2.30	6.50	7.10	8.90	11.1

DLS measurement of MK-2 containing AOT/isooctane RMs.

Dynamic Light Scattering (DLS) confirmed the formation of reverse micelles. Samples of MK-2 RMs were prepared in 0.10 M AOT/isooctane and the results are shown in Table A2. The

Table A2. DLS measurements on MK-2 in 0.10 M AOT/isooctane RMs
[a]Radius measurements were taken from the volume distribution
[b]Maitra, A. *J. Phys. Chem.* **1984,** *88,* 5122-5125

W_O	[RM] (mM)	MK-2 r_h[a] (nm)	PDI MK-2 RM	Empty r_h[a] (nm)	PDI Empty RM	Lit. r_h[b] (nm)
4	1.0	2.0 (±0.60)	0.13	2.1 (±1.1)	0.20	2.5
8	1.5	2.8 (±0.94)	0.18	3.1 (±2.0)	0.17	3.2
12	2.7	3.5 (±1.0)	0.18	3.4 (±2.0)	0.13	3.7
16	5.1	4.1 (±1.2)	0.20	4.0 (±2.0)	0.22	4.2
20	11	4.6 (±1.2)	0.16	4.1 (±2.0)	0.34	4.4

average radius obtained from w_0 sizes 4 through 20 compared favorably with those reported previously in the literature.[16, 55, 56] These results were observed with RMs prepared with and

without MK-2. These results showed that RMs formed, and that the presence of MK-2 did not significantly affect the size of the reverse micelle.